Wesleyan University

Gas Phase Spectroscopy of 4⁻aminophenethyl Alcohol and Clusters with Carboxylic Acids

By:

Caitlin Bray

Faculty Advisor: Dr. Joseph L. Knee

A Dissertation submitted to the Faculty of Wesleyan University in partial fulfillment of the requirements for the degree of Master of the Arts

Middletown, Connecticut December 2015

Abstract:

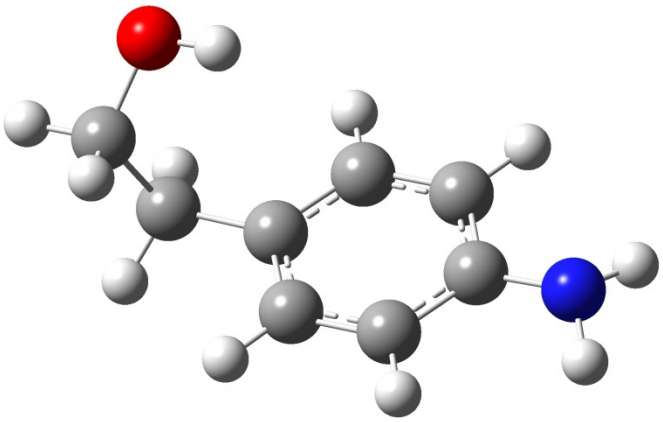

4–aminophenethyl Alcohol (4-AE)

Both ultraviolet and infrared laser spectroscopy methods were used to study the structure of 4-aminophenethyl alcohol, 4-AE, and its formic, acetic, and propionic acid clusters. The “floppy” side chain of the 4–AE molecule is capable of forming different conformational isomers. The 4–AE molecule has both an amine and a hydroxyl functional group which are potential sites for hydrogen bonding with the acids. The acids are all carboxylic acids which were able to form a one-to-one cluster with the 4–AE through hydrogen bonding with the 4–AE acting as a base. Through quantum chemical calculations using DFT methods and measurements of the S_1 excited state using ultraviolet techniques and of the S_0 state using IR-UV double resonance techniques determination of the structure of 4–AE and its clusters was achieved. Frequency shifts of the origin of the S_1 excited state and the –OH stretches of the S_0 ground state were used in the structural determination.

Table of Figures:

Table of Tables:

Table of Contents

Introduction:

Jet-cooled laser spectroscopy has become a widely used technique for studying basic properties of molecules. Both ultraviolet, UV, and infrared, IR, regions are easily accessible with lasers and are in the frequency range for studying electronic and vibrational transitions in many molecules and clusters. Jet-cooled supersonic expansion cools and isolates gas phase molecules, which greatly simplifies the spectra, to be studied in high-resolution experiments.

Room temperature molecules have a large amount of excess energy. The high temperature of the molecules results in many vibrational and rotational states being populated. This multitude of states complicates the spectra causing many overlapping peaks with large peak widths. Cooling the molecules reduces the excess energy in the molecules and a majority of the molecules settle into a single vibrational state and a limited rotational state distribution. The cooling of the gas molecules is done through supersonic jet expansion. A carrier gas is used to mix with the vapors of the molecule of interest then expands out into the vacuum chamber and through a skimmer to the form a collimated molecular beam. The molecules are cooled as the gas expands through collisions with the backing gas. The molecule is effectively cooled to about 1 K rotationally and the translational velocity distribution is narrowed through these collisions resulting in a more uniform molecular beam.[1] The vibrational cooling is more complex and higher, non-boltzman, vibrational temperatures are expected. The width of the experimental peaks give an indication of the level of rotational cooling

achieved in the beam and the existence of hot bands indicates the degree of vibrational cooling. The choice of backing gas effects the vibrational cooling due to the gas velocity. Helium, which is a common backing gas, is a small atom with a high velocity which results in higher vibrational temperatures compared to heavier and slower noble gases such as argon.[2]

In order to undergo cooling all the molecules of study must be in the gas phase. This can limit the molecules of study to molecules which can be achieved in the high enough concentration in the gas phase. Heating the samples of interest can help increase vapor pressure for liquids or solids of interest expanding the molecules for potential study. The gas phase molecules are in a vacuum limiting the total number of molecules present in the experiment. Interactions between molecules in the experiment are limited because the experiment is done in a vacuum in the gas phase. Solvent effects and other intermolecular forces are minimized which limits the number of variables in the experiment and simplifies the interpretation of results.

The molecules most amenable to study in our laboratory contain aromatic groups which lead to electronic transitions which are often strong, and in the lower energy region of the UV spectrum accessible to the available lasers. Molecules which absorb light and enter the excited state in the visible range are called chromophores. All of the molecules studied are chromophores because the electronic transition is accessible with the lasers allowing the vibrational structure to be studied. Many of the molecules studied have rigid aromatic structures with “floppy” side chains. These

side chains allow different interactions and properties to be probed through laser spectroscopy. Hydroxyl groups, carboxylic acids, amines, and carbon chains all can be side chains of a chromophore providing the opportunity to explore their properties. Small clusters formed in the supersonic jet expansion can be studied from the point of view of the chromophore in the cluster. In this way, the interaction between a chromophore with other small molecules such as water, argon, formic acid, and methanol can be studied. Clusters of different sizes can be formed and studied, such as a chromophore with one, two, three, or four water molecules such as the analysis done by Gu on 4-aminophenethyl alcohol.[3]

The range of molecules which can be studied has expanded as experimental and computational advances have been made allowing larger, more complex molecules to be studied. The complexities of the vibrational structure as well as the difficulty of getting some molecules into the gas phase are obstacles which are constantly faced when choosing a molecule of study. The Zwier group has done many conformational studied on “floppy” molecules such as sinapate ester derivatives and leucine encephalin. Clusters studied by the Zwier group include dipheoxxyethane and water clusters and dilignols with alkali metal clusters.[4,5,6,7] Other groups have studied biologically relevant molecules such as tryptophan and guanine.[8,9,10] The study of interactions and some biologically relevant molecules in the gas phase is an avenue for isolated and simplified study of the molecules of interest.

Conformational studies of “floppy” molecules and weakly bound clusters are often subjects of interest. A “floppy” molecule is one which can be reasonably considered to exist in equilibrium of multiple conformations with significant population at standard conditions. Our group has recently explored the interactions of acids and bases in gas phase clusters. Previously 9-fluorenemethanol and alcohols, aniline argon complexes, and 9-hydroxy-9-fluorenecarboxylic acid, 9HFCA, complexes have all been studied by Knee et. al.[11,12,13,14] Conformational studies focus on the existence of multiple possible conformations and the identification of the conformations observed in experimentation. The cooling process of the molecular beam can “freeze out” the different conformations preserving the room temperature equilibrium in the molecular beam. This may happen when the vibrational energy is lowered below the barrier of conversion between the conformations. The room temperature equilibrium can be preserved through this cooling depending on the barrier height, effective vibrational cooling, and equilibrium allowing the study to reflect what is naturally observed at room temperature.

In previous studies the chromophore, 9HFCA served as the acid in the study of the acid base interactions. To further explore these acid base interactions, 4-AE is used as the base in hydrogen bonded clusters and is paired with a variety of carboxylic acids. The acids used for experiments were formic, acetic, and propionic acid. Each of these acids has the same basic structure with slightly different acidity and carbon chain length. The hydrogen bonding site of the acids is identical so any differences in the cluster structure can be accounted to acidity or length of the carbon

chain. The gas phase acidities of these acids are listed below in the table showing the range of acidities explored in the experiments.

Acid	Structure	pK_a	Gas Phase Acidity (kcal/mol)	Mass
Formic	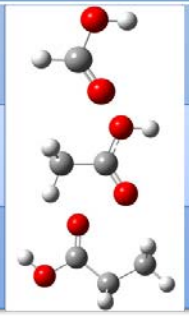	3.75	338.6	46
Acetic		4.76	341.5	60
Propionic		4.88	340.4	72

Table 1: The carboxylic acids used in the experiments are shown in the above table. The gas phase acidity and chain length are the variable features of the acids.

The presence of –OH stretches in the acid base interactions is one of the reasons that these interactions are of interest. The ground state vibration of the –OH stretches are accessible using infrared techniques and are strong infrared absorbers. The strong infrared signal is important for the technically difficult infrared experiments to be successful. Complexes of acid base interactions are hydrogen bonded and often involve a hydroxyl group. The –OH stretches shift based on the environmental conditions of the molecule and the binding of the –OH. The frequency of the –OH stretch is indicative of the strength of the –OH bond. A weakening of the –OH bond shifts the frequency to the red and broadens the band. The measured –OH stretch frequency can be used to aid in structural determination of the clusters by comparison to calculations and information can be gained about the estimated strength of the hydrogen bonds. The different shifts of the –OH stretch, depending on

the bonding of the clusters, are important clues for considering the cluster structure and connectivity.

The study of the 4-AE with the carboxylic acids is an opportunity to study the acid base interactions from the point of view of the base. The previous studies were done with an acid chromophore and binding partners of a base. The conformational studies of the clusters with the simple carboxylic acids only include one chromophore and changes in the system can only be viewed from the point of view of the 4-AE. Gaining information about 4-AE and other bases which are chromophores is needed to explore the option of clusters with two chromophores. Specifically the carboxylic like 9HFCA is a good binding partner for a chromophore base which would allow the cluster to be viewed from the perspective of the acid and the base to observe the similarities and differences in the spectra of both chromophores of the cluster.

In conjunction with experimental methods, calculations have become an instrumental tool in understanding the basic properties and interactions of molecules. Quantum chemical calculations are based on solving the Schrödinger equation. Calculations are able to aid in the determination of relative energies of conformers, vibrational frequencies, ionization potentials, and binding energies in clusters. At a very basic level, quantum mechanical calculations aid in visualizing and gaining a qualitative understanding of the molecular system being studied. More detail and information on chemical calculations is explained in the calculations section.

Background:

Vibrational laser spectroscopy in the ultraviolet and infrared ranges is an important probe for understanding structure and bonding of molecules. Our group has focused on hydrogen bonded structures and understanding the role of multiple conformations in the systems of study. The molecule of interest for this study is 4-aminophenethyl alcohol, 4-AE. As is required, 4-AE is a chromophore and thus will absorb photons to give off a signal in our chamber. Past studies in our group have focused on a carboxylic acid chromophore with a variety of bases or water. These systems have studied the hydrogen bonding in clusters from the point of view of the carboxylic acid. The current study focuses on a system of a base with carboxylic acids reversing the roles so that the chromophore, 4-AE, is the base.

4-AE has been used in some experimentation in the functionalization of graphene nanoplatelets, for preparation of ordered poly (amide-ester) and uses in synthesis but no molecular spectroscopy studies of 4-AE were found in the literature. The formation of clusters with 4-AE and carboxylic acids can be theoretically formed in multiple ways. The amine and hydroxyl group are both potential hydrogen acceptors. The electron rich aromatic ring also has the potential to participate in the hydrogen bonding and strengthen the cluster binding energy.

Previous work by our group has been done on 4-AE. Preliminary studies on the molecule were performed by Gu. This work included some calculations at the B3LYP level using Gaussian 09 of the monomer, monomer and one formic acid

clusters, and monomer and water clusters. In addition to computational studies, some ultraviolet measurements were taken. The monomer was characterized using resonance enhanced multi-photon Ionization (REMPI) techniques. The identification of a second conformation of the monomer was explored using MATI, mass analyzed threshold ionization. The calculations suggest the presence of a second conformation is present and by comparing the MATI signal of the first few peaks in the REMPI scan a second conformation was identified. Complexes with water were also explored. Both REMPI and UV-UV hole burning experiments were done to understand the 4-AE and water complexes up to four waters. The work with the formic acid includes only the initial REMPI scan. The work presented in this thesis is an extension of these initial results to include additional acid binding partners and the application of infra-red spectroscopy to better understand the detailed bonding interactions which occur in these chapters.

The goal is to expand the study of 4-AE and understand how it interacts and bonds with carboxylic acids. This is an extension of previous work and falls in line with the work the group has done in the past. Ultimately a study of chromophores including both carboxylic acids and bases will allow clusters of two chromophores to be studied. The hydrogen bonds between the clusters could then be probed from both the acid and base perspective and form a complete picture of the system. Working with 4-AE to understand how it hydrogen bonds and finding the frequency ranges is a step to understanding the hydrogen bonding from the perspective of a base.

Experimental:

A variety of techniques were employed to study 4-AE. Different laser spectroscopy experiments and quantum calculations were used to help understand and characterize 4-AE and its acid clusters. Utilizing both the ultraviolet, UV, and infrared, IR, regions of the spectrum provided a large amount of information on the molecules. The same basic set-up of the chamber and electronics were employed for all these experiments. Differences in laser timing and frequency among other specifics are described separately for each experiment.

All experiments were conducted using a vacuum chamber with two compartments. A diagram of the chamber is included in Figure 1.The front chamber is connected to a 6" diffusion pump and kept a pressure of approximately 10^{-4} torr. The front compartment houses the pulsed nozzle and the sample container. The sample container is a small steel reservoir that is located before the nozzle. A bolt on the top of the sample container allows the container to be opened to put in a new sample and keeps an airtight path for the gas to flow. The sample is typically held in a small glass test tube in the sample container. The bottom of an NMR tube is the appropriate size. Placing the sample in the tube allowed for easier clean-up of the sample container and minimized the contamination of samples. A backing gas of helium is flowed through the lines and over the sample container before reaching the nozzle. The vapors of the sample are then picked up and carried in the gas. The pressure of the backing gas was varied to optimize the signal conditions for individual

experiments but was between 20 and 30 psi. The nozzle has an orifice diameter of about 0.8 mm and is a General Valve series 9 pulsed valve. A plastic poppet is used in the pulsed valve and needs to be replaced over time due to mechanical deformation and from exposure to high heat. The value is opened by a solenoid actuator whose timing is controlled by a pulse carefully timed to the laser firing. After leaving the nozzle, the gas enters the chamber and undergoes a supersonic expansion. Collisions between the sample and the backing gas result in a molecular uniform translational speed. The sample is rotationally and vibrationally cooled through these collisions. The pulsed valve minimizes the amount of sample and backing gas that is put into the chamber when compared to a continuous stream nozzle. The pulsed value is fired approximately 4.13 msec before the lasers fire to allow for the delay in the opening of the nozzle and the transit time of molecules from the nozzle to the interaction region, approximately 100 μsec.

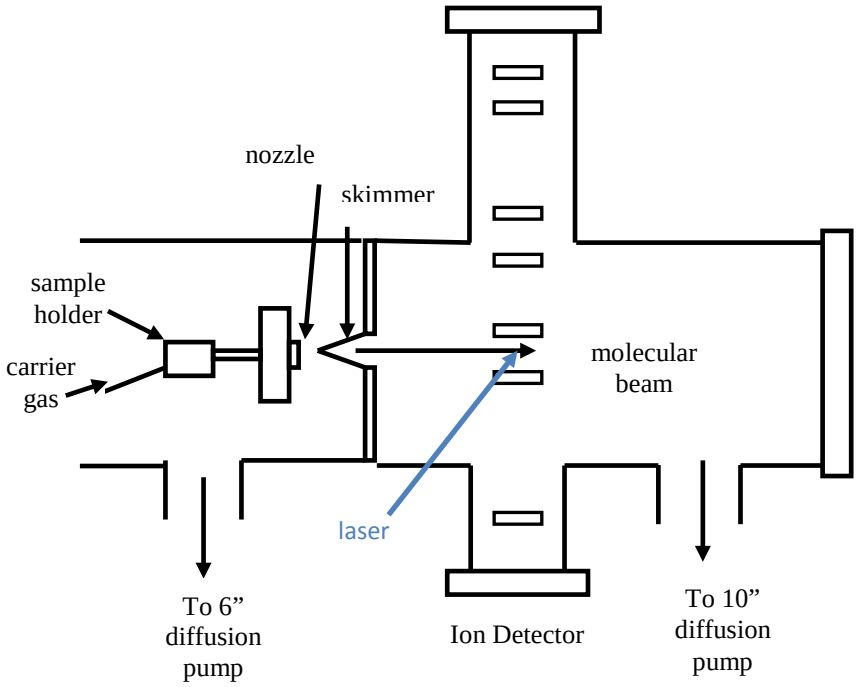

Figure 1: A diagram of the vacuum chamber showing the nozzle, sample container, skimmer, and intersection of the laser and molecular beam between the electric fields as it is in our experimental set-up.

Both the nozzle and the sample container are connected to thermocouples and resistive heaters. External controls of the heaters allow the temperature to be varied for different experiments and compounds. The temperature can be monitored during the experiment and changed as necessary using these controls. The nozzle is always kept at a higher temperature than the sample container to avoid condensation of any material on the nozzle as the gas passes through. Heating of the sample container inside of the vacuum chamber controls the vapor pressure of the sample which is usually a solid with low vapor pressure at room temperature. As a result we are able to measure spectra from chromophores which are liquids and solids with low vapor pressures by heating them to increase the vapor pressure. The nozzle can also be used

to hold sample. This results in a higher signal level but also uses the sample much more quickly and requires opening the chamber to replace the sample more often. The short lifetime of the sample and regular cleaning can help avoid sample degradation. For the 4-AE, we found that there was ample amount of monomer signal using the sample container and did not need to put sample in the nozzle. Placing sample in the nozzle can also be done so that another compound can be put in the sample container allowing two compounds with low vapor pressures to be simultaneously used.

The backing gas used for all the experiments is helium. The helium runs through the external lines where the pressure and flow rate can be regulated. The lines split the gas into two paths. One path is clean and goes directly into the chamber. The other line runs over an external sample container. The external sample container is used for studies of clusters. The external container is used for compounds with high vapor pressures. By leaving the container at room temperature or placing it on ice the vapor pressure can be regulated in a simple way. Acids and water are both put into this container when cluster studies are being studied. The line that runs through the sample container recombines with the pure gas and enters the chamber. The flow rate of the two separate lines can be controlled using a flow meter. This limits the amount of sample mixed with the backing gas from the external container.

The two compartments of the vacuum chamber are separated by a wall and the molecular beam is allowed to pass from the front chamber to the back chamber through a skimmer. The skimmer is shaped like a cone with a hole at the point which

is pointed towards the nozzle and is used to collimate the molecular beam before it enters into the back chamber where it will be intersected with the lasers for measurement. The nozzle can be moved to better align with the skimmer. Experimentally it was found that better signal was achieved when the nozzle was closer to the skimmer, usually within one centimeter of the skimmer.

The back chamber houses the time-of-flight mass spectrometer and detector. The laser beams pass through windows into the back chamber where they intersect with the molecular beam in the extraction region of the mass spectrometer. The back chamber is connected to a 10" diffusion pump and is typically kept at a pressure of about 10^{-6} torr as measured by an ion gauge. There are three transmissive grid electrodes within the chamber an upper, middle, and lower grid. All the experiments conducted collected ions and thus had a similar field set-up. The ion extraction and collection of ions can be done in either a static or pulsed scheme. In both cases three potentials are used and applied to three grids as shown in Figure 2. The extraction potentials used follow the Wiley and McClaren scheme in order to optimized the mass resolution of the spectrometer.[15] For the static extraction scheme the upper grid, or repeller, was set at +3500 V, the middle grid was set at +2800 V, and the lower grid was grounded, 0 V. In this scheme when the ions are created they accelerate downward toward the detector and after passing through the lower grid travel through a field free region until they approach the microchannel plate, MCP, detector. The detector face is set to -2500 V which accelerates the ions to impact with significant energy. Upon impact, electrons are ejected which are then accelerated to a second

plate which provides further amplification with these electrons before continuing to the detector anode which is held at ground. The electron current at the anode is the signal collected which is directed to an oscilloscope. The overall gain of the detector is greater than 10^6.

In addition to the electric field configuration described above, a pulsed extraction was used for some experiments. The set-up for the pulsed extraction only exhibits a change on the upper grid. The upper grid is set to alternate between a low voltage and a higher voltage. The high voltage used is +3500V which is the same as the voltage of the upper grid in the original configuration. The low voltage used on the upper grid is about +1000V but can be changed to optimize the peak width as long as it remains lower than the voltage on the middle grid. The upper grid rests at the lower voltage and is pulsed to the higher voltage with a large pulse width, one microsecond. The pulse is timed using a delay after the laser is fired. Using a pulsed extraction can alter the arrival time of the ions to the detector and also increase the time of flight of the ions. The pulse is off when the ions are created and so the ions drift upwards away from the higher positive electric field below it. Once the extraction pulse is on, the ions go back down towards the detector because of the increased positive charge on the upper grid. A longer flight time can help to narrow peaks. Two color hole burning experiments take advantage of the ability to reverse the mass arrival. The burn laser can be set to interact with the molecular beam while the pulse is off and then the probe laser interacts with the beam as the pulse turns on so that the ions created by the probe see the higher positively charged grid and have

less distance to travel than the ions created earlier so they arrive first despite being created second. The expected small intensity of the signal created by the probe laser will not be interfered or mixed with the larger intensity of the burn laser when the probe ions arrive first.

The detector can be used to either detect ions or electrons based on the set-up. A power supply provides the charge on the face of the detector and outputs data to the oscilloscope. The tube extending below the chamber holds the electric fields and is the time of flight tube for the apparatus. The molecular beam passes between the upper and middle grid where it is intersected with the laser beams creating ions. The ions are then guided by electric fields to the detector. The upper grid has the highest positive voltage and repels the ions downward. The time of flight of the ions is directly proportional to their mass causing the heavier ions arrive later than the lighter ions. As a result the detector has mass resolution based on the arrival time of the ions. The information is then processed and displayed on the oscilloscope. The mass resolution is very fine and peaks from naturally occurring isotopes, such as those found in chlorine and bromine, have been observed. The mass resolution is key to the experiments for ensuring the correct data is being observed and for differentiating between clusters and molecules. It is also possible to get an idea of the number of clusters being formed by observing both the one-to-one cluster as well as looking for larger clusters. It should also be noted that larger clusters can dissociate when ionized and fall into a lower mass channel while still maintaining the vibrational signature of the larger cluster.

Mass resolution of the observed peaks is important for ensuring measurement of the correct signal. Despite experiments being conducted in a vacuum chamber, water can get into the experiment and cluster with the monomer. Additionally residues from previous experiments can linger in the chamber and produce signals on the oscilloscope. Mass resolution on the oscilloscope separates out these peaks and determines the correct peak to measure. A flight tube is attached to the chamber and using electric fields to guide the ions, causes separation in the arrival time of the ions based on mass. The following equation[15] can be used as an approximation of the time-of-flight for an ion of given mass, m. In the below equation, m is the mass of the compound, τ is the arrival time of the associated peak on the oscilloscope, U is the energy of the ion, and D is the distance the ion travels in the field free region of the flight tube.

$$\tau = 1.02(2m)^{1/2}\frac{D}{2U^{1/2}}$$

This equation can be further simplified using experimentally known masses and times of arrival to easily predict the time of arrival of other masses using the following equation. The below equation combines constants and assigns them to a value of c to give a rough estimate of the time of arrival based on a given mass.

$$c = \frac{\tau^2}{m}$$

The constant c is determined based on experimental data of a known peak. Identifying one known peak on the oscilloscope is enough to use the above equation to predict

the mass of the other shown peaks or the expected position of a given molecule. A longer flight tube has a longer time of flight and provides greater mass separation. A reflectron is a type of flight tube that redirects the ions using electric fields so that twice the path length is achieved and the effect of redirection by the electric fields further separates the ions by mass.[16] Research on a reflectron to further improve the mass separation has been done and a reflectron can be implemented.

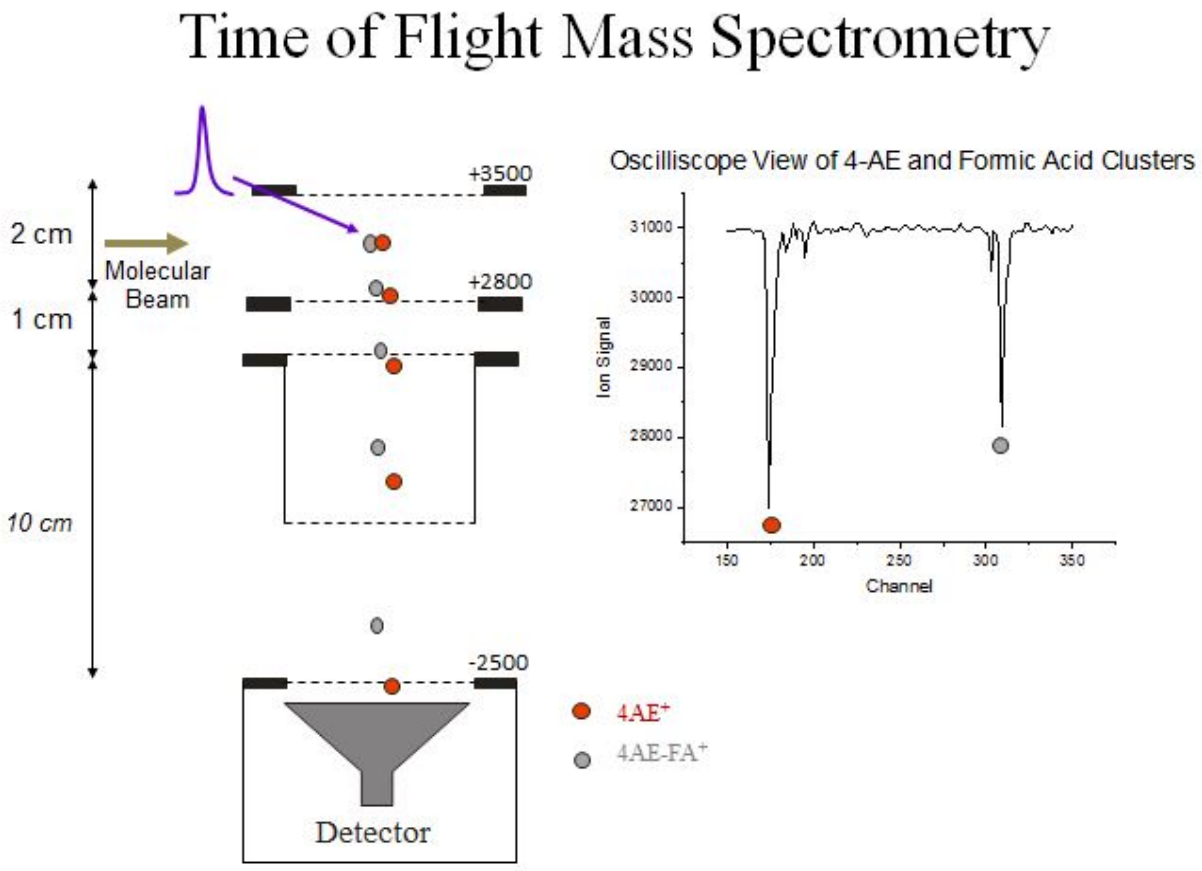

Figure 2: The above figure includes a diagram of the mass spectrometry and a snapshot of the oscilloscope at a resonance of the formic acid cluster. The diagram shows the configuration of the electric fields and the detector in relation to the area of interaction.

There are two lasers used for these experiments. One is a nanosecond pulsed Nd:YAG laser (Continuum) which produced light at 532nm which is used to pump a dye laser (Lumonics HD500). The dye laser produces tunable light across the visible spectrum. The visible pulses from the dye laser are then frequency doubled (WEX Spectra Physics) providing approximately 1 millijoule per pulse in the ultraviolet. The pulsed YAG laser runs at a frequency of 20Hz with a pulse width of approximately 10 nsec. The other laser is also a pulsed Nd:YAG laser (Continuum Precision) also operating at 20 Hz with a pulse width of approximately 10 nsec. The 532nm pulses are then used to pump a dye laser (Quanta-Ray PDL) which is then frequency doubled (WEX Spectra Physics) to provide approximately 1 millijoule per pulse.

The experiments in this thesis all characterize 4-AE. 4-AE is a solid compound with a low vapor pressure. Through experimental testing it was found that heating the 4-AE to 95°C resulted in the best monomer signal level. Higher temperatures approach the melting point of 4-AE and will melt the sample. High temperatures increase the amount of monomer sample causing monomer clusters and large fragmentation of the monomer signal. The monomer was tested in both the nozzle and sample container for best signal level and it was found that using the sample container was most advantageous. The high level of signal achievable, up to 1V, using the sample container was more than sufficient to conduct experiments. Using 4-AE in the nozzle provided small increases in signal level but required replacing the same and opening the chamber frequently. Therefore, the experiments were all run with 4-AE in the sample container set to 95°C and with the nozzle empty

and set at 100°C to avoid condensation of the sample in the nozzle or connecting tubing. The acids, propionic, acetic, and formic, used in the cluster experiments were all liquids with high vapor pressures and were put in the sample container outside of the chamber. Experiments with water were also done using the sample container outside the chamber. Propionic has the lowest vapor pressure of all of these and was left a room temperature. The other acids and water all had vapor pressures too high at room temperature and the sample container was surrounded with ice to cut back the vapor pressure. Flow rates for each of these were optimized independently to maximize the 1-1 cluster and minimize the larger clusters.

A variety of experiments were used to gain an understanding of the 4-AE monomer and hydrogen bonded clusters. The techniques used in this thesis are resonance enhanced multiphoton ionization (REMPI) and infrared (IR) experiments. Hole burning experiments with two ultraviolet wavelengths as well as with ultraviolet and infrared wavelengths were also conducted.

REMPI experiments were used as an initial probe to get information about the monomer and clusters via electronic spectroscopy. The one color REMPI experiments were first used to find the origin of the first excited state, S_1, of the monomer or cluster. This technique uses one laser to pump and probe the molecule. The laser beam intersects with the molecular beam in the back compartment of the vacuum chamber between the grids of the mass spectrometer as shown in Figure 2. The first photon absorbed by the molecule excites it from the S_0 state, ground state, to the S_1

state, excited state. A second photon of the same energy is then absorbed by the molecule. This second photon has enough energy to ionize the molecule. Then the positively charged ion is collected by the mass spectrometer as described above. The key to this experiment is the energy of the first photon absorbed by the molecule will only excite the molecule if the energy of the photon exactly matches the energy required to excite the molecule from its current state to an energy level in the excited state, or in other words there is a resonance at the particular wavelength. The population of the v=0 vibration in the ground state has the greatest population and it is thus assumed that this is the starting state of the excited molecules. The peak farthest to the red, excluding hot bands, is the origin peak marking the transition from the S_0 v=0 vibration to the S_1 v=0 excited state. Peaks to the red of the origin are hotbands and are the excitation of S_0 state molecules

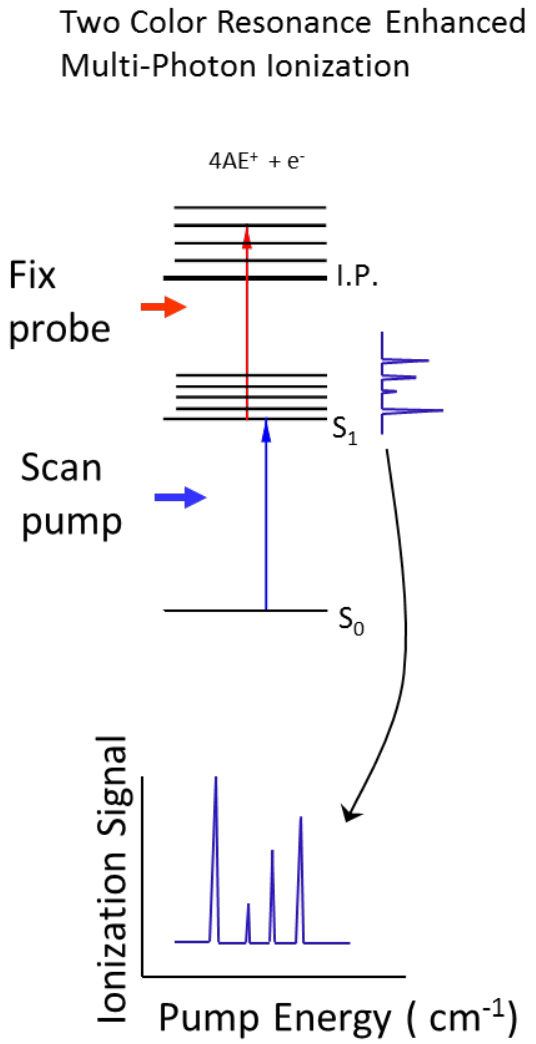

Figure 3: Energy diagram for REMPI experiment scheme. The resulting spectrum is a measurement of the energy of the excitation energy as measured by the pump laser. The above picture shows a two color REMPI experiment.

in higher vibrational states to the S_1 excited state. Beyond the origin are peaks to the blue which are excitations of the ground state to higher vibrational levels of the excited state. The resulting REMPI spectrum is a measure of the excited S_1 state of the molecule with the peaks representing the energy of transitions from the ground state to the excited state and its vibrations.

Two color REMPI experiments were also conducted. The two color experiments use two lasers, one as the probe and one as the pump. The probe is scanned over the desired wavelength range to excite the molecule from the ground state to the S_1 excited state. The pump is set at a wavelength that is confidently over the ionization potential of the molecule of interest but below the origin peak wavelength this disallows the pump laser from producing signal independent of the probe. The pump laser is the second photon in the experiment and will ionize the already excited molecule. The lasers are temporarily separated so that the probe comes first and is followed by the pump. Spatially the lasers are overlapped so that both beams are sampling the part of the molecular beam. Two color REMPI experiments are generally less noisy and produce cleaner scans. This comes from the fact that there is less excess energy in the system and thus fewer possibilities for decay or conversion of species which can produce noise in the spectrum. The goal of the REMPI experiments is to gain information about the S_1 excited state and also to get an initial handle on the molecule of study through the origin peak. The mass resolution of the technique is critical because it allows easy separation of the contribution from the monomer or possible clusters in the beam.

The monomer and clusters may have multiple conformations coming from different local minima on the ground state potential energy surface. Depending on the barrier height between conformations, the room temperature equilibrium, and the degree of vibrational cooling in the molecular beam, these multiple conformations may be observed in experimentation. To explore this possibility, hole burning experiments are often done. The resonant wavelengths of origin and vibrational peaks are at different wavelengths for separate conformations because of the different energy landscape of the conformations. Hole burning experiments are two color experiments. The first color is the burn laser. This laser is set to a resonant wavelength for the molecule to excite a significant number of molecules with the vibration corresponding to the selected wavelength. This “burns” out many of the molecules with the same conformation as the selected peak targeted by the burn laser. Stating that all these molecules are burned out is equivalent to stating that they are excited and ionized by the burn laser so that they are no longer available for interaction with the second laser. The second laser is delayed by five to ten nanoseconds and then is used to do a one color REMPI scan of the remaining molecules. Both lasers are sampling the same portion of the molecular beam so the second laser is only able to interact with the remaining molecules that were not preciously ionized by the burn laser. As a result the signal produced by the second laser only includes molecules with a different conformation than those depleted by the first laser. A result of no signal from the second laser would suggest a second conformation is not present in the molecular beam. The scan can be done using an

"on vs off" subtraction to improve the background noise and maintain a consistent baseline. The subtraction alternates taking data points with and without the burn laser present so that the resulting difference will be a reflection of the change in signal induced by the burn laser. This experiment works well for separating out two different conformations that have similar energies and are in the same wavelength region. The amount of signal produced is also a factor in the success of these experiments to ensure the signal can be clearly discerned compared to the baseline.

Infrared experiments pump the ground state vibrations of the molecule and are instrumental in identifying the correct ground state structure. The IR experiments pose a greater technical challenge and careful set-up but once completed provide information on the unique vibrations of the ground state. The energy diagram of the IR experiments, as shown in Figure 4, is very similar to that of the UV experiments. These experiments are two color experiments. The beams are spatially overlapped and temporally separated by about 20 nanoseconds such that the beams are both sampling the same region of the molecular beam. The second color is the probe and is tuned to the origin peak of the molecule. The pump is in the ultraviolet range and excites and

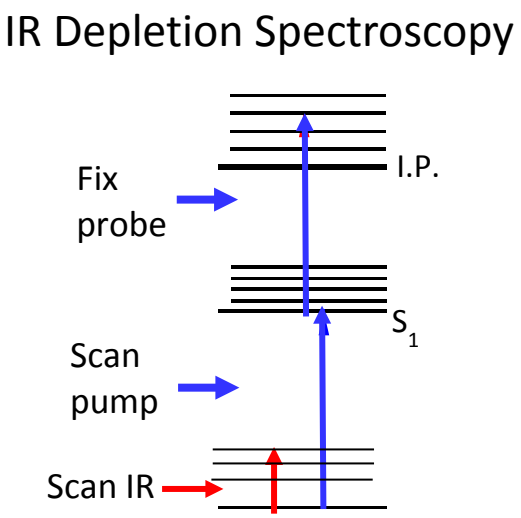

Figure 4: An energy diagram depicting the IR depletion scan scheme. The signal that results from this experiment is a depletion of the one color REMPI signal which is collected from the beams in blue. The red line is the IR energy which is depleting the ground state of the molecule as it hits the frequencies of ground state vibrations.

ionizes the molecules like a one color REMPI scan. The oscilloscope displays the signal level for the ions collected from the one color REMPI scan. The first color, the infrared beam, arrives before the ultraviolet beam and is the probe. The pump is in the infrared range which allows it to probe for vibrational excitations in the ground state. The pump is scanned over a region to look for a ground state vibration of the molecule which is observed by a depletion of the REMPI signal produced by the probe. When the pump laser hits the specific frequency of a ground state vibration the molecules are vibrationally excited in the S_0 state and no longer interact with the probe laser causing a depletion of the signal level from the probe. The absorption of the IR wavelength cause the molecules to no longer be in the same energy state and are therefore not available for the chosen ultraviolet transition. Because the observance of a vibration is measured by depletion of the REMPI signal, these vibrations are specific to the conformation being probed by the ultraviolet laser. IR experiments provide conformer specific information about the ground state of a molecule or cluster. Hole burning studies using infrared frequencies as a burn laser can also be done. The IR studies done in this thesis focused on the hydroxyl stretch region of the infrared spectrum, around 3600 cm^{-1}. The monomer has one hydroxyl stretch while the clusters have the 4–AE hydroxyl stretch along with the acid stretch. Shifts in these stretches are of interest to understand the strength and structure of the hydrogen bonding in the clusters.

In addition to experimentation, quantum mechanical calculations are an important tool for analyzing the properties of the molecules. To complement the

experimental methods, *ab initio* and quantum mechanical methods were used to calculate predicted structures, energies, and vibrations. The Gaussian ’09 suite and the Wesleyan Cluster were used to perform these calculations. B3LYP calculations were the main source of information used though M0-62X and MP2 functionals were explored. The calculations are particularly important in visualizing and determining the minimum structures of the monomer and clusters. Identifying these structures can be done in tandem with the vibrational data.

Calculations:

The use of quantum mechanical calculations has become a standard complement to experimental studies in physical chemistry. Geometry optimization, energy and frequency calculations are of particular interest for the investigation of the structure and interactions of 4-AE and acid binding partners. Vibrational spectroscopy focuses on the quantum mechanical properties of the molecule to determine the bonding and structure of the molecule. Calculations provide an important tool in assisting the analysis of experimental data and are generally accurate in their own right.

There are many different approaches to calculations using different methods and basis sets. Hartree-Fock Theory, Semi-empirical methods, Moller-Plesset (MP) Perturbation Theory, and Density Function Theory (DFT) are commonly applied by computational programs.[17] The semi-empirical methods are based on parameterization from experimental data and are the quickest and least accurate methods available. Because semi-empirical methods are built using experimental data, the methods are generally optimized for a specific category of molecules and perform well for those molecules which fall into the same category used to optimize the system. Hartree-Fock Theory is the most simplistic and fastest approach that attempts to solve the Schrödinger Equation and is employed for large molecular systems. The speed and computational power of current computers allows more complex methods to be used for many molecules and interactions. Moller-Plesset

Perturbation Theory is known to be more accurate than the Hartree-Fock Theory but is significantly more computationally demanding, expensive. Perturbation theory attempts to build on Hartree-Fock theory by applying small perturbations to the solution to get a more accurate solution. Density Functional Theory, DFT, uses general functionals of the electron density to model the behavior of the molecule.[17] The results achieved are comparable to Moller-Plesset Theory's accuracy with a significant decrease in computational time. Density Functional Theory is constantly improving and evolving as new functionals are developed and has proven to be a reliable method. DFT methods have been developed to model electron interactions and as a result certain methods have been optimized to model certain chemical interactions such as noncovalent interactions, barrier heights, or main group thermochemistry. A careful choice of DFT method can provide very reliable results.

Two density functional methods were used, B3LYP and M06-2X. The B3LYP method is a very popular density functional and is a hybrid GGA, generalized gradient approximation, method. The B3LYP method is composed of the Becke 88 exchange function and the Lee-Yang-Parr correlation function.[18,19] The M06-2X method is relatively new and was developed by Truhlar et al. It is a hybrid meta-GGA method and has been shown to perform well in cases of hydrogen bonding.[20] The M06-2X method differs from the B3LYP method in the amount of exact exchange included in the functional. B3LYP employs the original three parameters and values originally developed by Becke while M06-2X empirically fit the parameter values. The M06-2X method has been used by our group previously and proven to work well

for our hydrogen bonded systems of study. All calculations were done using a Pople Basis set 6-311G++(d,p). This basis set is a split valence basis set with polarization and diffuse functions.[21] The density functional methods with this large basis set provide a balance between accuracy and computational power.

A series of calculations on the 4-AE and the clusters were done using the Gaussian 09 suite.[22] The Wesleyan University computer cluster supported by the NSF under grant number CNS-0619508 was used for the computations. A variety of methods, B3LYP, MP2 and M06-2X, were used in exploratory studies to best understand what was going on and to compare to the experimental data. The differences found between methods used were small considering that the calculations were primarily used for qualitative studies and estimations of energies.

The main purpose of the calculations is to understand the minimum energy structures and to predict the frequencies of vibrations in the structures. Both the 4-AE and 4-AE acid clusters were studied using calculations to predict this information. The 4-AE monomer is a ring based structure with some flexibility in the side chains. An aromatic six membered ring is the base of the 4-AE structure. An amino group is connected to the ring and has some flexibility in the position of the hydrogens of the amino group. The other side chain is para to the amino group and features a two carbon chain with a hydroxyl group at the end. Rotations and movement by this hydroxyl group are the main cause of energy differences between possible structures of the monomer.

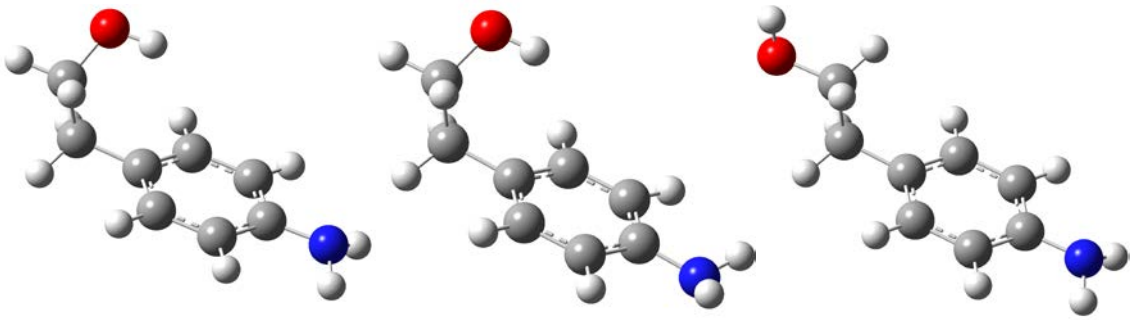

Figure 5: The three 4-AE minimum energy conformations. From left to right, the gauche, flipped, and anti conformation of the monomer.

The calculations revealed three minimum energy conformations as shown in Figure 5. Of the three conformations the minimum energy conformation had the hydrogens on the amine pointed down below the plane created by the ring and the carbon chain with the hydroxyl group above the plane the ring. The hydroxyl group is positioned over the ring in a gauche position. For this reason the minimum energy conformation is referred to as the gauche conformation. The next lowest energy conformation is mainly the same structure with the hydrogens on the amine group flipped such that they are now above the plane of the ring. This structure will be referred to as the flipped structure. Finally the third local minimum energy structure considered has the hydrogens on the amine pointed down below the plane of the ring and the hydroxyl group pointed away from the ring completely anti to the amine group. This structure is referred to as the anti conformation.

These three structures considered were chosen from a larger group of local minima that were predicted by the calculations. The B3LYP calculations were used as

the primary source of information for analysis and comparison throughout experimentation. The following energy calculations are all given from the predicted energies from the B3LYP calculations. The gauche conformation was the lowest energy with a predicted energy of -441.5789729 hartrees. This conformation is the reference point that all other monomer conformations is compared to because it's energy is predicted to be the lowest and we were able to confirm that it is the main conformation we see in experimentation. The position of the hydroxyl group allows it to interact with the electron rich aromatic ring. The high electron density in close to proximity to the basic hydroxyl group can form a weak intramolecular bond stabilizing the structure. The next lowest energy conformation is the flipped conformation and is 15 cm^{-1} higher in energy than the gauche conformation. This is not a surprise since the flipped structure is very similar to the gauche conformation and the main stabilization of the gauche structure comes from the position of the hydroxyl group over the ring. The flipped structure is almost identical to the gauche conformation and the stabilization from the position of the hydroxyl group is not changed. On the other hand the anti conformation is a rotation of the hydroxyl group and is 322 cm^{-1} higher in energy than the gauche conformation. The predicted IR frequencies of the –OH stretch in the monomer further support the idea that the stabilization of the molecule comes from the proximity of the hydroxyl group to the aromatic ring and will be discussed later. The energy calculations of the structure do clearly relate the position of the hydroxyl group and the predicted energy.

Both MP2 and M06-2X calculations were explored as calculational methods to check for consistency and understand the biases of the methods used to predict the structure. The energies are shown in Table **2**. The M06-2X method has been used previously in the Knee group with great success and MP2 methods are known to be of good accuracy. All methods were in agreement of the minimum energy structure of gauche. The difference between the gauche and the anti conformation varied for the different methods. The MP2 and M06-2X predicted the gauche conformation to be 601 cm^{-1} and 633 cm^{-1} lower respectively. The structures predicted for the monomer were verified and considered to be good estimations of the expected potential structures.

4AE Energy	Gauche (au)	Anti (au)	Difference (cm^{-1})
B3LYP	-441.5789729	-441.577051	322
M06-2X	-441.3822677	-441.3793834	633
MP2	-440.290576	-440.2878371	601

Table 2: The calculated energies of the two main monomer conformations considered using different computational methods.

The main study focuses on the hydrogen bonding structure between the 4-AE and a variety of acids. The acids studied were formic, acetic, and propionic acid. Modeling of the hydrogen bonded structures included many possibilities to explore in the search for a minimum energy structure. The studies were mainly done using B3LYP calculations with the MP2 and M06-2X calculations used for comparison with some selected geometries. Both the gauche and the anti conformation were used

as a starting point in the search for the minimum energy structures of the clusters. Hydrogen bonding sites on both the amine and the hydroxyl group were explicitly explored. In the searches of the hydroxyl group's hydrogen bonding some interaction with the aromatic ring of the structure was seen and in this way was considered as a possible hydrogen bonding site.

Some common themes popped up in the calculations and predicted structures of the acid clusters. All of the predicted lowest energy structures used the gauche monomer structure. This is not a surprise since the gauche conformation was the lower energy structure of the monomer. The gauche structure has stability from intramolecular bonds between the ring and the hydroxyl group. The high electron density surrounding the hydroxyl group makes the oxygen of the hydroxyl group a better hydrogen acceptor and can more readily react with the acid to form a hydrogen bond. The anti conformation is higher in energy and doesn't feature this intramolecular behavior to facilitate the hydrogen bonding of the hydroxyl with the acid. The energy difference in the structures pointed to the monomer in the gauche state for every acid cluster. Experimentally, there is more opportunity for the acids to cluster with the gauche monomer and barring any rearrangements it would be expected the clusters would feature the gauche conformation of the monomer because of the higher population of the gauche conformation in the molecular beam. Further analysis of the acid cluster structures and experiments all focused on the gauche monomer for this reason.

Within the gauche conformation there are multiple possibilities for hydrogen bonding of the acid and the monomer. The structures that hydrogen bonded to the amine group were predicted to be significantly higher in energy for all of the acid clusters. Excluding some extensive searches for a propionic and 4-AE cluster structure, explicit binding with the aromatic ring system of the 4-AE was not explored. As a result, the hydrogen bonding with the carboxylic acid was believed to occur with the hydroxyl group. The main focus and hypothesized hydrogen bonded structure concentrated on the interaction between the hydroxyl group of the monomer and the acids. All the acids in the experiment are carboxylic acids and thus have two oxygens and a hydrogen which may participate in intermolecular bonding with the 4⁻AE.

Two competing minimum energy structures were predicted for the clusters of the gauche conformation. The predicted difference in energy between the two structures varied based on the computational method used and the acid in the cluster. Experimentation is necessary to confirm any prediction on the structure of the clusters. The two structures of the clusters considered are referred to as gauche and ring and are shown in Figure **6**. The gauche conformation is with the gauche monomer and the carboxylic acid interacting solely with the hydroxyl group in hydrogen bonding. The acid points away from the rest of the 4-AE molecule and forms a psuedo-six membered ring of interaction between the three oxygens and hydrogens in the interacting groups. In the ring conformation the monomer is again in the gauche conformation and the acid interacts with the hydroxyl group on the

monomer. The difference is that the hydrogen in the hydroxyl group of the monomer does not interact with the oxygen of the acid. The bonding site of the acid is almost perpendicular to the hydroxyl group. The hydrogen on the 4-AE hydroxyl group continues to weakly interact with the aromatic character of the ring instead. The hydrogen on the ring closest to the acid is closer to the oxygen of the carboxylic acid and can weakly interact with the oxygen becoming the sixth member of the psuedo-six membered ring.

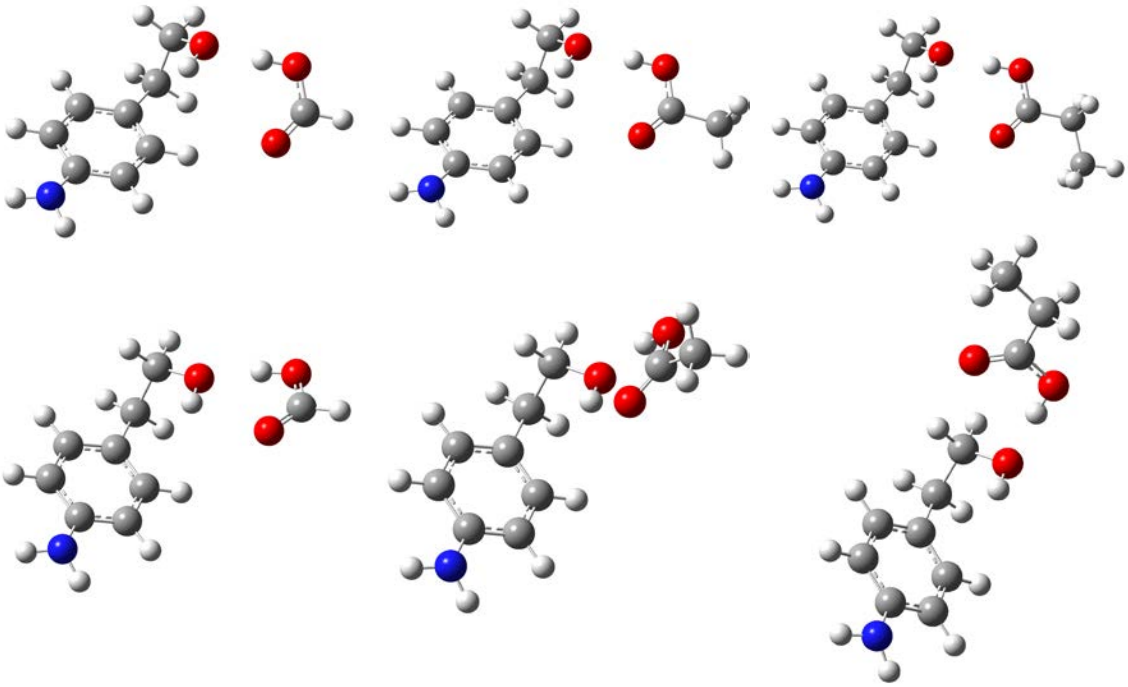

Figure 6: Cluster conformations for all three acids. The top row is the ring conformation and the bottom row is the gauche conformation. The main difference between the conformations is the rotation of the acid in relation to the hydroxyl group of the monomer. The ring structure has the acid perpendicular to the hydroxyl group where the gauche structure has the acid parallel to the hydroxyl group. The columns are the different acids, from left to right formic, acetic, and propionic acid.

The propionic acid cluster appeared to be different from the formic and acetic clusters in experimentation which required explanation. The previous calculations predicted that all the structures would be similar and only very small differences from

acidity and carbon chain length were seen. To try and find a solution or explanation another look into the possible structures was attempted by running more calculations to search for local minima. Using the B3LYP method, the geometry optimization settled on to the two structures mentioned above for all of the acids. Branching out to other methods different potential conformations were seen. The ring structure is a local minima structure using all of the methods and deserves consideration for all of the acids. The gauche conformation shown in Figure 6 is the result of the B3LYP geometry optimization; the other methods shifted the acid into another position. A different predicted minima energy structure is found for both the acetic acid and the propionic acid with the acid over the aromatic ring of the 4⁻AE. The B3LYP method will not converge on this other structure but it could be found using both the MP2 and M06-2X methods. This structure is the gauche monomer with the acid over the ring of the 4⁻AE. The hydrogen bonding interaction appears to occur only between the carboxylic acid and the hydroxyl group of the monomer. Using the M06-2X method the structure is predicted to be much lower in energy, 405 cm^{-1} lower than the gauche conformation, a binding energy of about 500 cm^{-1} greater and to have a distinct infrared spectrum for the –OH stretches. Figure 7 shows the over the ring structure of

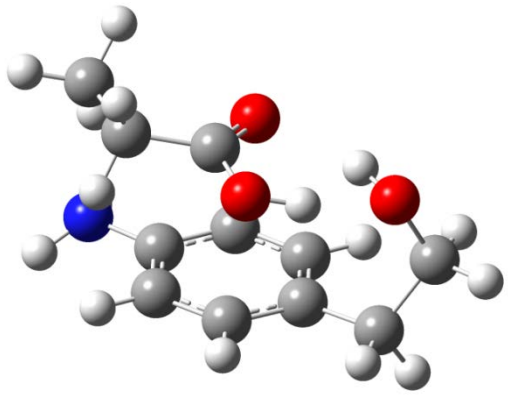

Figure 7: Shown above is the over the ring structure of the propionic cluster which resulted from calculations using both the M06-2X and MP2 methods.

the propionic acid and 4⁻AE. Other structures were also found using the B3LYP method but were predicted to be much higher in energy and therefore an unlikely conformation of the cluster. The exploration of further clusters is an important consideration to understanding what is occurring in the propionic cluster. Potential structures of the clusters are considered with the experimental results to determine the cluster conformations.

By comparing the energy of the cluster structure and the two separated molecules, an estimate of the binding energy was determined. For all the estimated cluster structures the estimated binding energy was over 3,200 cm^{-1}; the exact values for the estimates are listed in Table **3** . Consistent with the energy calculations which generally predicted higher energy structures for the clusters using the B3LYP method, the predicted binding energy of the B3LYP structures was much lower than the same structures calculated with MP2 or M06-2X. These two methods predicted binding energies closer to 4,400 cm^{-1} for all the clusters. The predicted binding energies were above the highest predicted frequency of the –OH stretch measured suggesting the cluster would not dissociate upon IR excitation.

cm^{-1}	Gauche	Ring	Anti
Formic Acid	-3357.4	-3327.5	-3662.0
Acetic Acid	-3260.0	-3254.2	-3580.2
Propionic Acid	-3220.4	-3221.17	-3266.6

Table 3: The calculated binding energies for the cluster conformations using the energies from the B3LYP calculations. All of the binding energies predict a considerable stabilization energy of the cluster.

In addition to structure and energy considerations, vibrational frequencies are of interest since they can report directly on the bonding interactions which occur upon complexation. We are most interested in the -OH stretches in the molecules. This is because they are generally strong, are at experimentally accessible frequencies, and are directly involved with the hydrogen bonding interaction that we are trying to characterize and understand. Calculated frequencies were used for the monomer and clusters to aid in finding the infrared signals of the molecule and to confirm the identification of these signals as -OH stretches.

Frequency calculations were done on all the potential structures explored. An appropriate scaling factor should be applied to all of the frequency calculations. The B3LYP/6-311++G(d, p) method has been used in our group with infrared experiments. Using experimental data on –OH stretches with 9HFCA and calculations on the system with the same method, a scaling factor of 0.952 was determined to be correct for the –OH stretches.[13] Applying this factor to the current system gives results which are shown to be very close to the experimentally measured frequencies for the –OH stretches. Predicting the position of the infrared frequencies is important for setting up the IR experiments and understanding the range over which to expect the –OH stretches. The cluster structures are held together primarily by interactions between the monomer –OH group and the acid. The strength of the hydrogen bonded interaction and the bonding partner effect the frequency of the –OH stretch which is shifted from the 4-AE hydroxyl stretch in all cases. The relative shifts of different calculated structures are important for understanding and determining the

structure of the clusters. Other computational methods had not been compared to experiment in our group and so the B3LYP calculations were relied on for the frequency predictions.

Ring	AcidH-MonoO (Å)	Mono O-H (Å)	Mono –OH Stretch (cm^{-1})
Formic Acid	1.71568	0.96708	3584.58
Acetic Acid	1.73783	0.96707	3584.92
Propionic Acid	1.74341	0.96694	3585.51

Table 4: Ring cluster conformation measurements of the bond lengths in the primary hydrogen bonding interaction and the predicted frequency of the 4⁻AE –OH stretch. The frequency is scaled by a factor of 0.952

Gauche	AcidH-MonoO (Å)	Mono O-H (Å)	Mono –OH Stretch (cm^{-1})
Formic Acid	1.71905	0.96807	3577.72
Acetic Acid	1.74766	0.97144	3521.87
Propionic Acid	1.75148	0.97130	3523.98

Table 5: Gauche cluster conformation measurements of the bond lengths in the primary hydrogen bonding interaction and the predicted frequency of the 4⁻AE –OH stretch. The frequency is scaled by a factor of 0.952

The structure of the cluster plays a key role in the frequency of the –OH stretch. The 4⁻AE monomer has the highest frequency of the –OH stretch as expected because the –OH bond is strongest in the monomer. The gauche and anti monomer structures have different predicted –OH frequencies because of the difference in the hydroxyl position. The monomer anti conformation frequency is predicted to be at 3842 cm^{-1} which is about 40 cm^{-1} to the blue of the predicted the gauche

conformation monomer –OH stretch. This supports the hypothesis that the gauche conformation is lower in energy because the electron rich aromatic ring can interact with the hydroxyl group stabilizing it. This stabilization would weaken the –OH bond and lower the expected frequency compared to the anti conformation which is predicted by the calculations. All the clusters include an interaction with the 4⁻AE hydroxyl group weakening the bond to the hydrogen and red shifting the expected frequency of the –OH stretch. The above tables, Table **4** and Table **5**, list the distances between atoms at the acid/base interaction site and the predicted monomer ⁻OH stretch. The similarities in the distances confirm that the same interaction is present in each of the predicted structures and the structures are similar as they visually appear to be. The distances between the acidic hydrogen and monomer oxygen of the hydroxyl group is an indication of the strength of the acid/base interaction. In all cases the distance is shorter for the formic acid suggesting a stronger interaction. The bond length of the monomer hydroxyl group is an indication of the strength of the bond which affects the monomer ⁻OH stretch. Figure **8** shows the plotted IR predictions for the structures to compare the locations of the IR stretches. The ring and gauche structures have slightly different predictions for the frequency of the 4⁻AE –OH stretch. For the ring structure, all three acids are predicted to have 4⁻AE –OH stretches within one wavenumber of each other. The bond length, and therefore strength, of the 4⁻AE –OH bond is also predicted to be very close to each other for all three acids in the optimized ring structure of the clusters. The gauche structures predict that the 4⁻AE –OH stretches to all be slightly

farther to the red suggesting a stronger interaction of the acid with the hydroxyl group. The propionic and acetic acid, which have very similar gas phase acidities, are predicted to be two wavenumbers apart while the formic acid is 60 wavenumbers to the blue of the acetic and propionic. In both the ring and gauche structure the formic acid 4⁻AE –OH stretch is predicted to be in a very similar location. The position of the formic cluster 4⁻AE –OH stretch relative to the acetic and propionic stretches can thus be used to evaluate the expected structure of the clusters.

The acid clusters have a second –OH stretch which can be measured. This is the –OH stretch of the acid. The hydrogen in the bond is the acidic hydrogen and so upon cluster formation the hydrogen donation weakens the covalent –OH bond leading to a reduced stretch frequency expected to be around to 3200 cm^{-1}. The intensity of the predicted peaks is much greater than the expected intensity of the –OH stretches of the monomer. The relative position of these peaks can also be used to help predict the structure of the cluster but as will be noted later, the experimental conditions in this range were difficult and the acid –OH stretches can be used as supporting information but were not used as primary evidence of the cluster structure.

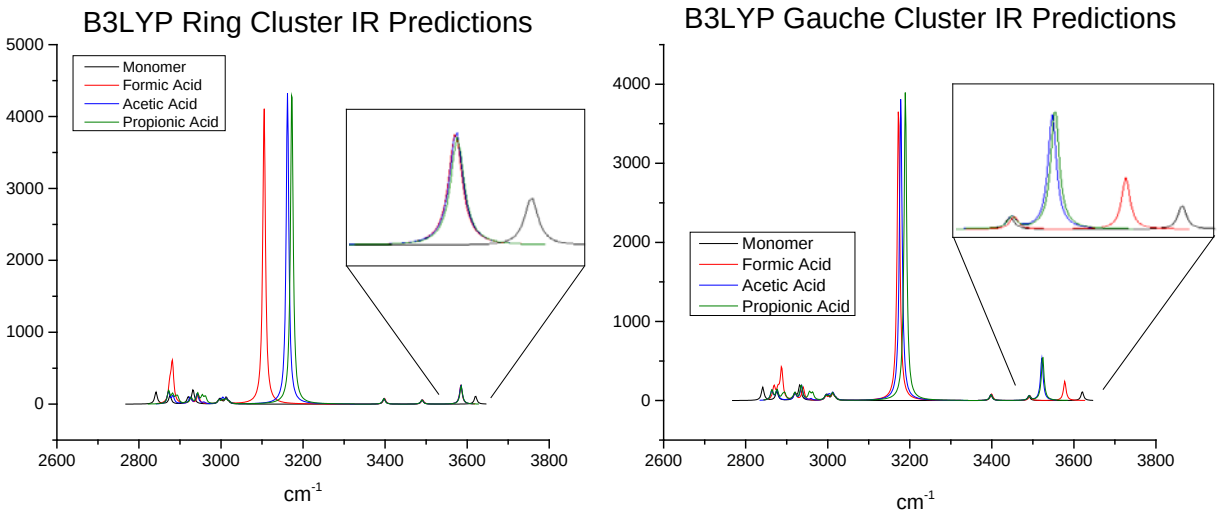

Figure 8: Above are two graphs depicting the predicted IR frequencies of the –OH stretches as well as other vibrations for the ring structure and for the gauche structure. The 4-AE -OH peak of the predicted IR spectra is the bluest peak of the spectrum for each cluster considered. The largest peak close to 3200 is the acid -OH peak. The calculated IR spectra are scaled by a factor of 0.952.

Calculations provide a large amount of information about the clusters and 4-AE monomer which can be verified through experiment. Employing quantum mechanical calculations has become a key fixture of spectroscopy and is important for understanding the molecule and clusters. The methods chosen were DFT methods which have been proven to predict vibrations and geometries well. The calculations provided a way to think about the structures of the molecules and to understand where to expect peaks in the IR experiments. Overall the calculations provide a basic understanding of the guiding interactions and possible structures of the clusters and the monomer but confirmation of the predicted structures must come from experimentation.

Results & Discussion:

The first experiments were done on the 4-AE monomer to determine the conformations present in the beam. Due to changes required in the experimental set-up when switching between UV and IR scans, all of the UV experiments were done before any of the IR scans were attempted. In addition it is necessary to find the origin transition of the molecule of study before any other experiments can be done. An initial one-color REMPI scan of the monomer was taken and is shown in Figure 9. Each peak in the scan is positioned at a frequency which correlates to an excitation energy of the S_0 ground state to a vibration in the S_1 excited state. A vast majority of the molecules in the molecular beam are in the ground state. The first peak shown is then assumed to be at the frequency of the excitation energy from the S_0 v=0 state to the S_1 v=0 state. This is the lowest energy transition that can occur between the S_0 and S_1 state. The peak marking this transition is called the origin. The x-axis of the graph displays the energy in wavenumbers of the transition. The first photon absorbed by the molecule produces the transition to the excited state and the second photon ionizes the molecule so that the ion can be collected as a signal by the detector. Other peaks mark the transition from the ground state to a higher vibrational level in the S_1 excited state. These are generally of lower intensity than the origin peak because of less overlap of the wavefunction in the ground and excited state. Different conformations of a molecule will have different energy potentials and so the frequency of the transitions will be different. The geometry and energy levels of the conformation are generally similar enough that the signal from the two separate

conformations is expected to be in a similar frequency range. The ability to measure separate conformations is reliant upon the population of each conformation in the molecular beam; enough signal must be produced for the peaks to be observed above the noise level. For two separate conformations, two separate origins and associated vibrations are expected to be observed. A variety of techniques can be used to identify the peaks associated with a different conformation.

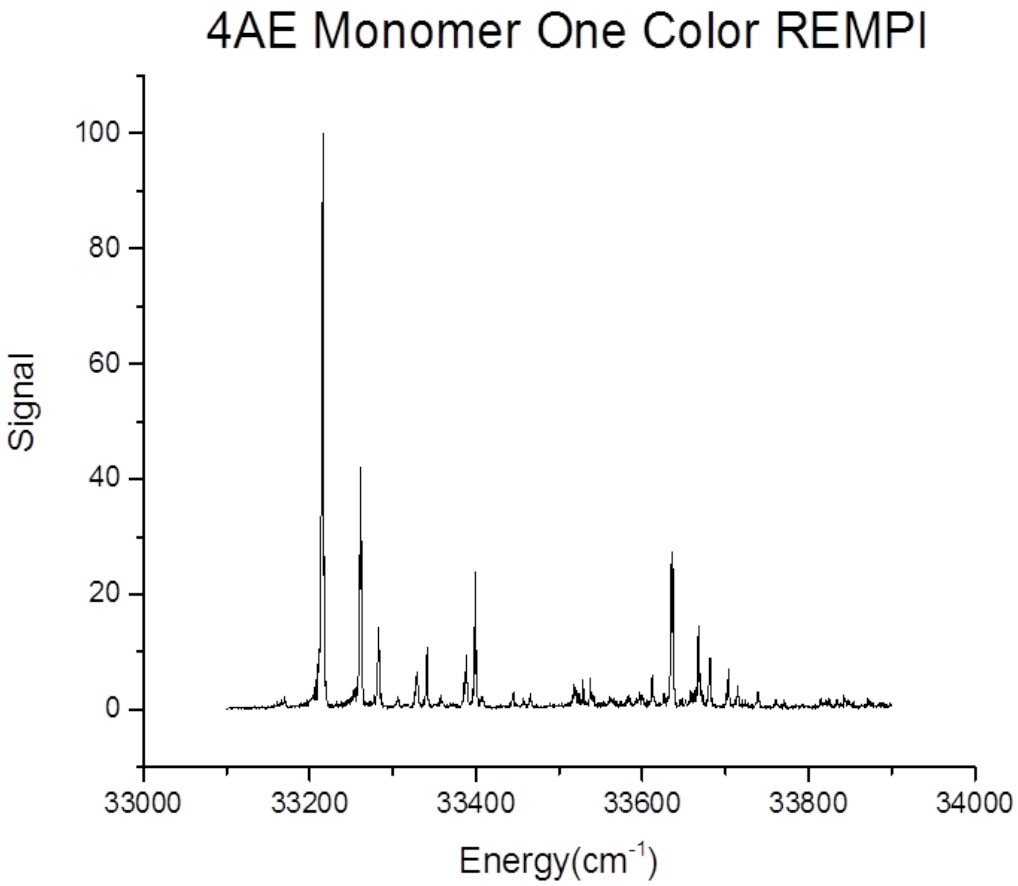

Figure 9: The spectrum is a one color REMPI spectrum of the 4-AE monomer. The large peak at 33215 cm^{-1} is the origin peak and the following peaks are vibrations. The x-axis is the wavelength of the $S_0 \rightarrow S_1$ excitation as measured by the scanning dye laser and the y-axis is a normalized measurement of the signal level measured by the detector.

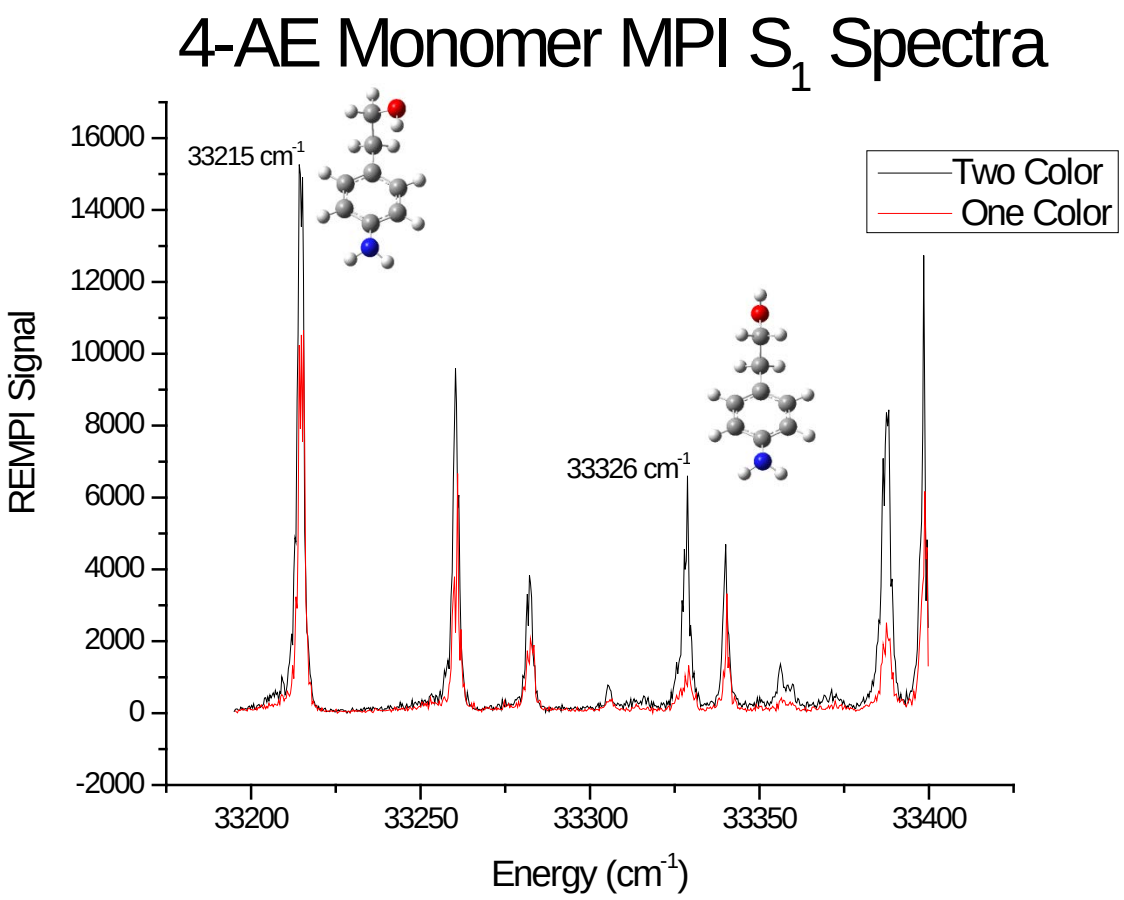

Figure 10: The one and two color REMPI scans are overlaid on top of each other to compare the relative enhancement of the peaks by the introduction of a second color. The second color is at a fixed wavelength and ionizes the excited molecules. The peak at 33326 cm^{-1} is an origin peak for a second monomer conformation.

Figure 10 shows the one color REMPI scan of the monomer overlaid with a two color scan. The peaks at 33,215 cm^{-1} and 33,326 cm^{-1} are assigned as the S_1 origin peaks for the gauche and anti conformations respectively. The peak at 33,215 cm^{-1} was assigned to the gauche conformation based on the greater total intensity of the origin and its associated vibrations. The gauche conformation is the lowest calculated energy conformation and is expected to be the most abundant. Previous data from Gu suggested another conformation at the 33,326 cm^{-1} peak. This was seen in our data through a two color REMPI experiment. Figure 10 shows a two color REMPI scan of 4-AE using 355 nm as the probing frequency. The peak at 33,326

cm^{-1} was enhanced by the probing significantly more than the origin identified at 33,215 cm^{-1}. The different enhancement level of the origin peaks suggests different photoionization energy for the two peaks. This led to the assignment of the anti origin at 33,326 cm^{-1}. A few of the other peaks also showed this preferential enhancement and are vibrations of the anti conformation. The anti conformation is a higher energy structure resulting in a smaller population of this conformation. A hole burning experiment was attempted next to solidify the evidence of the two conformations and to look for vibrations associated with the 33,326 cm^{-1} origin.

The hole burning of the 4-AE monomer was used to confirm the existence of two conformations of the 4-AE in the molecular beam and to determine which peaks are vibrations of the second conformation. The burn laser was set at 33,215 cm^{-1} to burn out the origin peak of the gauche conformation. In Figure 11 the results of the hole burning are shown. An “on vs off ” method was used to record the scan. The top graph in black is the resulting spectrum from only the probe laser when the burn laser was off. This spectrum is a one color REMPI scan of the 4-AE and so it includes all of the peaks seen regardless of conformation. The top black graph provides identical information to the graph in Figure 9. The red graph is the difference between the “on” and “off” states of the burn laser and so it is a representation of the intensity of signal from the molecules that were burned out by the burn laser. This is because when the burn laser is on the second color does not have a signal because there are no molecules left in the molecular beam that can be excited at the current wavelength. This red graph will only be a plot of the single conformation which was probed by the

burn laser and does not include any other peaks from other conformations. Dotted lines in Figure 11 point out the peaks which are missing from the difference graph. These are the peaks which can be assigned to the other conformation of 4-AE. The peak at 33,326 cm^{-1} is the reddest of the three peaks which were not burned. This confirms the assignment of this peak as a separate origin of the 4-AE. The peaks at 33383 cm^{-1} and 33697 cm^{-1} were also not burned and are thought to be the vibrations of the 33326 cm^{-1} origin.

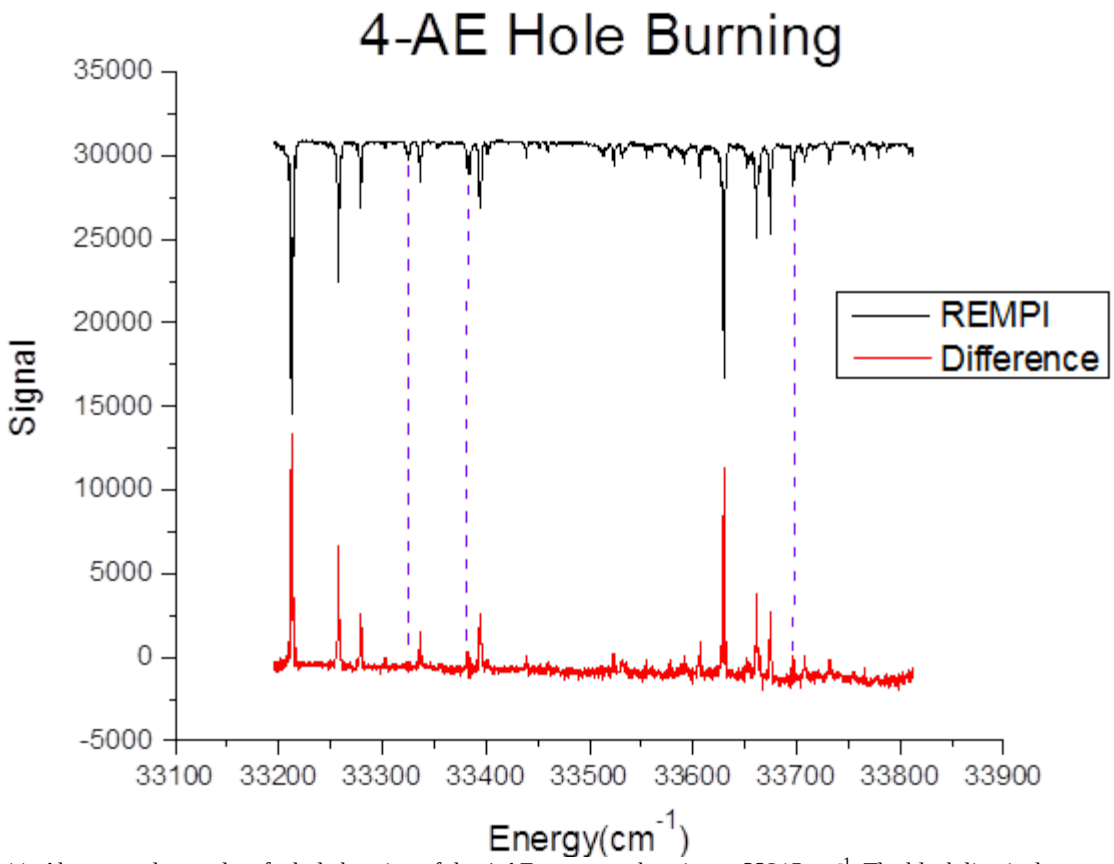

Figure 11: Above are the results of a hole burning of the 4-AE monomer burning at 33215 cm^{-1}. The black line is the one color REMPI spectrum collected when the burn laser was off. The red line is the result of subtracting the spectra collected when the burn laser was on from it was off. The result is the red line shows all of the intensity that was burned out by the burn laser.

The monomer IR studies were done to find a reference point for the cluster studies to help in determining the structure of the clusters. The infrared studies are a way to explore the ground state of the molecule. Unlike the UV studies which provide information on the excited state vibrations, the infrared wavelengths are able to probe vibrations in the ground state. The collection of signal requires the collection of ions and so excitation and ionization are still necessary to collect a signal. The IR studies are two color experiments. One color is set to the origin of the molecule of study. This color will excite and ionize the molecule producing a one color REMPI signal. The other color is the infrared light. The infrared is scanned over a region to find the ground state vibrations of the molecule. When the infrared is set to a wavelength corresponding to a ground state vibration the molecules in the ground state are vibrationally excited. The infrared beam arrives about one hundred nanoseconds before the ultraviolet beam. The lasers are spatially overlapped so that both lasers sample the same portion of the molecular beam. The early arrival of the infrared beam allows it to vibrationally excite the molecules so that they are no longer in the ground state and will not be excited and ionized by the ultraviolet beam. The amount of REMPI signal is monitored throughout the experiment as the IR is scanned over a region. Depletion of the signal indicated the position of a vibration in the ground state. IR studies were able to identify the –OH stretch of the free hydroxyl group in the gauche monomer.

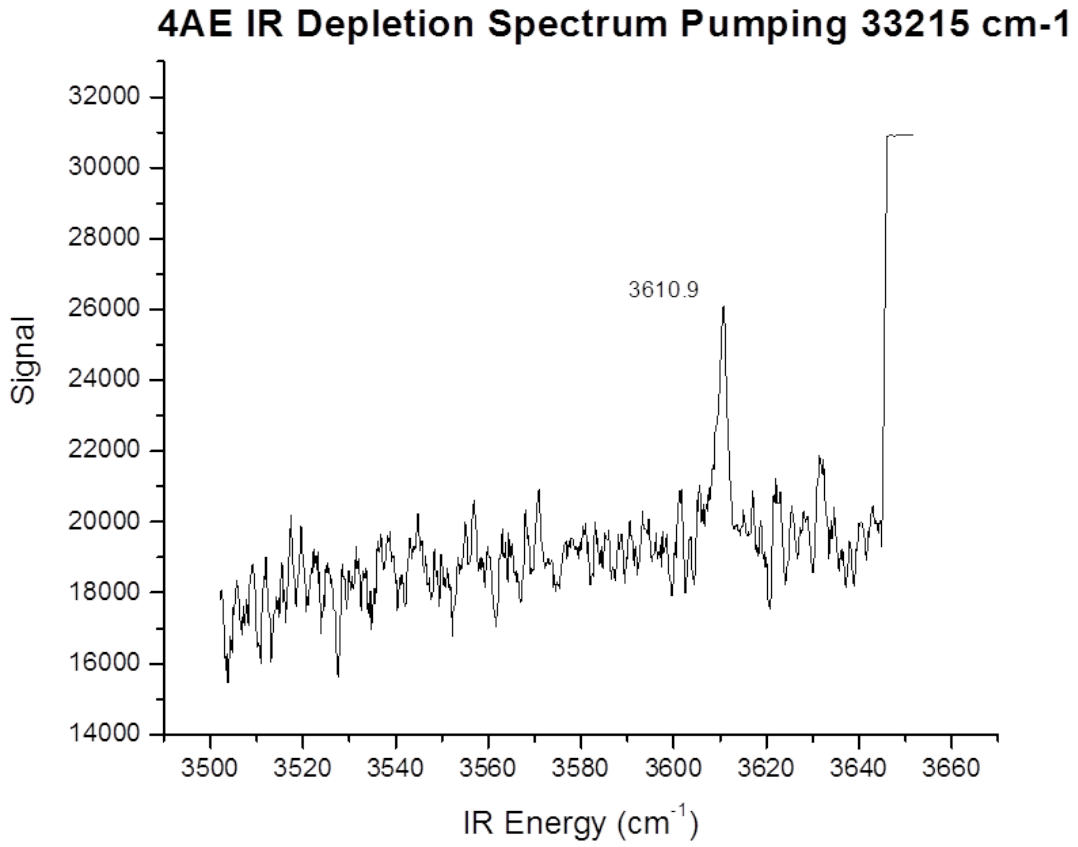

Figure 12: The infrared depletion spectrum of the gauche monomer conformation in the -OH stretch region. The 33215 cm^{-1} origin peak was probed with the UV laser. The top of the vertical line to the right shows the 100% depletion level.

The calculations suggest that two separate peaks for the gauche and anti conformations should be present and separated by about 40 cm^{-1}. Only the –OH stretch of the gauche conformation of the monomer was recorded. Calculations suggested the intensity of both the gauche and anti –OH stretch were similar with the anti peak being farther to the blue. The gauche peak was observed at 3,612 cm^{-1} with the probing laser at the gauche origin, 33,215 cm^{-1}. Figure 12 is the spectrum measured for the gauche 4-AE hydroxyl stretch. The flat line at the top right is the zero for no signal and the baseline is the full signal from the 4-AE REMPI. The peak at 3,610 cm^{-1} is the depletion of the REMPI signal due to the interaction between the

infrared frequency and the monomer. This peak is in the –OH stretch region of spectrum and is close to the scaled B3LYP prediction of 3,620 cm^{-1}. An attempt was made to measure the IR spectrum of the anti conformation by looking for depletion while probing the anti origin at 33,326 cm^{-1}. However no peaks were observed. This was likely due to the significantly smaller UV signal from the probe laser so that inadequate signal to noise prevented clear observation of the anti IR resonance.

The cluster experiments required more troubleshooting and adjustments than the monomer experiments. All of the acids were studied in both one and two color REMPI scans as well as infrared scans of both the monomer and acid hydroxyl stretch. The two color experiments were much cleaner for all the acids and are used instead of the one color REMPI scans. A comparison of the cluster and monomer REMPI scans is shown in Figure **13**. The two color scans use 355 nm as the second color for ionization of the electronically excited molecules. The 355 nm is lower in energy than the first color which would also ionize the molecule in a one color experiment. As a result there is less excess energy in the system and a clean signal and baseline can be achieved. The cluster calculations in some cases were less definitive in identifying the lowest energy conformation due to the existence of multiple, similar energy structures. In these cases calculations alone do not provide any solid basis for structure predictions and the expected structure is an open question. The experiments were technically more difficult as well because of an increase in variables. Each acid was unique and the smaller acids with higher vapor pressures proved easier to work with and draw conclusions about.

Formic acid is the smallest and most acidic of the acids studied. The high vapor pressure of the formic acid causes it to be easily mixed with the backing gas in relatively high concentration. The formic acid was placed in the side container on ice with a relatively low flow rate. The origin of the formic acid and 4-AE cluster is at 33,232 cm^{-1} which is blue shifted 17 cm^{-1} relative to the monomer. Hole burning experiments did not show any evidence of a second conformation and it is believed that there is only one conformation of the formic acid cluster in the molecular beam. This aligns with the results from the computational studies which predicted that the ring structure is much lower in energy than the other conformations considered. All methods of calculations predict the anti conformation to be greatly disfavored and the gauche structure to be between 160 and 170 cm^{-1} higher in energy than the ring structure. The ring structure is anticipated to be the structure of the cluster.

The acetic acid is the next acid in the series. The gas phase acidity of acetic acid is very similar to propionic acid, but is slightly less acidic making it the least acidic of the acids used in these experiments. The vapor pressure is still relatively high and the acetic acid was left in the sample container on ice to help cut back the amount of acetic acid entering the chamber. The 2:1cluster with the acetic acid could be seen but was minimized to have very low signal levels. The origin of the REMPI spectrum is at 33,248 cm^{-1} which is blue shifted from both the formic acid and the monomer origin. The blue shift is 33 cm^{-1} from the monomer origin. Hole burning experiments showed no evidence of a second conformation but based on calculations it is a possibility that there is a second conformation with a smaller population. The

calculations showed all the explored structures to be close in energy so it would be reasonable to expect two different conformations. The vibrational pattern of the acetic acid scan is much busier than the other scans which may conceal information about a second conformation with a small population.

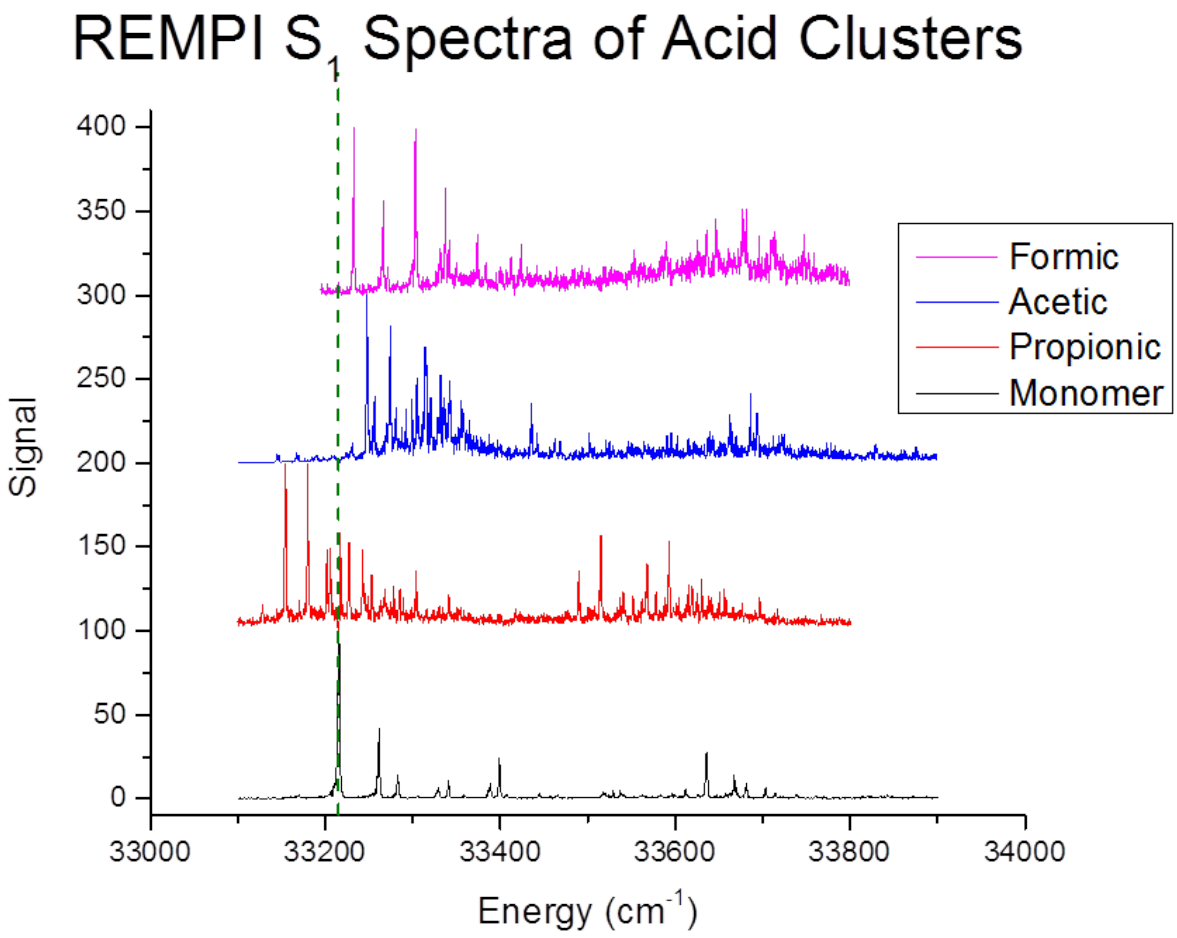

Figure 13: The figure compares the REMPI spectra of all the acid clusters and the monomer spectrum. The vertical green dotted line is a visual guide to look at the shifts of the acid cluster spectra compared to the monomer origin. Each of the spectra was normalized before plotting.

Propionic is the last acid that was used in the cluster studies. The propionic has the greatest mass and the lowest vapor pressure. Good signal levels were more difficult to achieve compared to the other acids and the propionic was at room temperature with a high flow rate. Unlike the previous two acids, the propionic acid has a red shifted origin relative to the monomer. The propionic cluster has its origin at 33,154 cm^{-1} which is red shifted by 61 cm^{-1}. This is a larger shift and a shift in the opposite direction of the other two acid clusters. Many calculations were done to explore the possibility of a different structure for the propionic acid to explain the difference in the shift. The minimum energy options were still the gauche and ring structures when the B3LYP method was used despite a large number of other structures that were explored. Using other methods, M06-2X and MP2, another structure was found that may be the structure of the propionic acid cluster. The main clues for determining the structure of the propionic acid will need to come from IR experiments. The results of the UV experiments suggest that the propionic interaction and thus cluster conformation is different from the other two acids and should be carefully considered.

The shift of the clusters' origins relative to the monomer origin provides information about the binding energy in the excited state. Calculations give an estimate of the binding energy in the ground state for each of the acid clusters. The binding energy is the stabilization energy gained from the formation of the cluster when compared to the two individual pieces, the 4-AE and the acid. The calculations are done for the ground state of the clusters and molecules so the binding energies are also for the ground state. All of the clusters have predicted binding energies, using B3LYP calculation, of over 3300 cm^{-1}. This is a considerable amount of stabilization energy in the ground state for the clusters. The REMPI spectra for the clusters is a measurement of the excited state and by comparing the shift of the origin peak with respect to the monomer the stabilization of the excited state can be considered. The origin peak is the measure of the lowest energy it takes to excite the cluster from the ground state to the excited

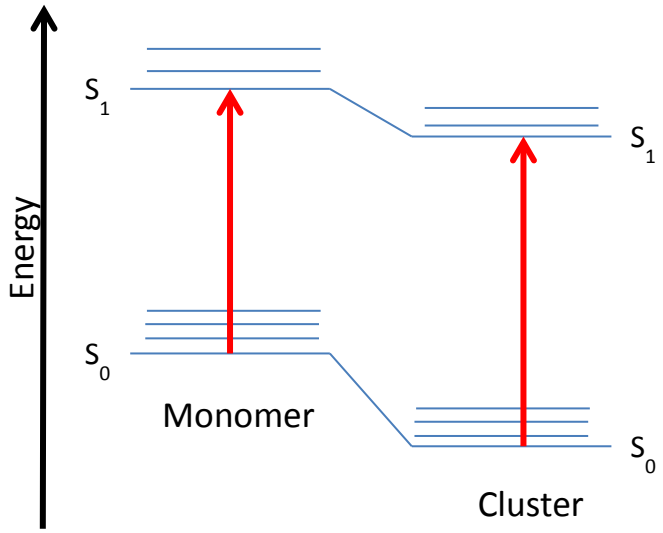

Figure 14: The ground state, S_0, of the cluster is stabilized compared to the monomer as shown by the strong binding energy of the clusters. This is depicted as a lower energy S_0 state for the cluster in the above diagram. The origin of the REMPI spectra for both cases determines the length of the red line which depicts the excitation of the ground state to the excited state. A shift in the cluster origin changes the length of the red line so that the excited state difference between the cluster and monomer is different from the ground state. Therefore the shift of the origin gives information about the relative stabilization of the excited state cluster compared to the monomer.

state. If the difference between the ground state and excited state energy was the same for the monomer and cluster complexes, the origin peak would be at the same wavelength for all of the molecules. This is not the case as the acid clusters shift relative to the monomer origin. The formic and acetic acid both blue shift relative to the monomer indicating that more energy is needed to excite them compared to the monomer and thus the difference between the ground and excited state is greater for these clusters. The increase in the energy difference between the ground and excited state for the clusters indicates the excited state must be closer in energy to the excited state monomer and so the cluster is not as well stabilized in the excited state as it is in the ground state. For example the formic acid has an experimental blue shift of 17 cm^{-1} and a calculated ground state estimated stabilization energy of 3327 cm^{-1} so the excited state cluster stabilization energy would be estimated to be 3310 cm^{-1}. The cluster can be assumed to be stabilized to some degree in the excited state or the cluster would dissociate in the excited state. The existence of the REMPI spectrum proves that the cluster is still present and must still be stabilized in the excited state but to a lesser degree as indicated by the blue shift. The propionic is different in that it has a red shifted origin. This indicates that the excited and ground state of the cluster are closer in energy when compared to the monomer and so the excited state must be more stabilized than the ground state for the propionic clusters. The opposite origin shift of the propionic is a key piece of evidence in suggesting that the propionic does not have the same cluster structure as the formic and acetic which are believed to both be in the ring structure. The propionic and acetic acid have very similar pKas and gas

phase acidities and so the bonded structure of the acid to the 4-AE monomer is the likely source of a difference in the two clusters. Red shifts of electronic transitions in clusters are quite common due the π to π^* nature of the aromatic chromophore excitation. The excited π electron is less tightly bound to the molecular core and more easily polarized leading to stronger dispersive interactions upon clustering.[23] Thus this red shift might imply there is more interaction of propionic acid with the π system then in the structure of the other acids.

Infrared studies were conducted on the monomer as well as the all the clusters. As previously mentioned the monomer study focused on only the main gauche conformation. The gauche conformation is the structure of the monomer in the clusters and the gauche conformation of the monomer will be used to determine the shift of the 4⁻AE hydroxyl stretch in the clusters. The frequency calculations from the B3LYP calculations were used to predict the experimental frequencies for the –OH stretches. The gauche cluster conformation calculations predict the acetic and propionic acid have the 4⁻AE –OH stretch in the same place and the 4⁻AE -OH stretch in the formic acid is more to the blue. The ring cluster conformation calculations predict that all of the acid clusters have the 4⁻AE –OH stretch at the same frequency.

The 4⁻AE –OH stretch in both the acetic and formic acid clusters were observed in the same position. Both spectrum are plotted together in Figure **15** to compare the position of the ⁻OH stretch depletion peak. The formic acid cluster 4⁻AE

–OH stretch was a sharp peak, width of about 5 cm^{-1}, at 3,563.5 cm^{-1}. The IR depletion spectrum showed about a 60% depletion of the cluster signal. Like the earlier monomer IR spectrum, the top of the vertical line on the left of the spectrum is the reference for 100% depletion and the baseline is with no depletion. The acetic acid cluster has the same frequency, 3,563.5 cm^{-1}, for the 4⁻AE –OH stretch but the signal is not as sharp. The peak is slightly broader, 7 cm^{-1}, than the formic cluster peak. The position of the 4⁻AE –OH stretch in both of the clusters confirms the ring structure as the correct structure for the formic and acetic acid clusters. The formic acid could be confidently expected to be in the ring form from the calculations. The acetic acid did not have a clear expected structure after considering the calculations but the gauche and the ring structure were the two main prospects. If either of the acid clusters had been in the gauche conformation, a separation of at least 8 cm^{-1} for the 4⁻AE –OH stretch would be expected. The identical position of the two ⁻OH stretches is solid evidence that the ring structure is the observed structure for the acetic and formic acid clusters.

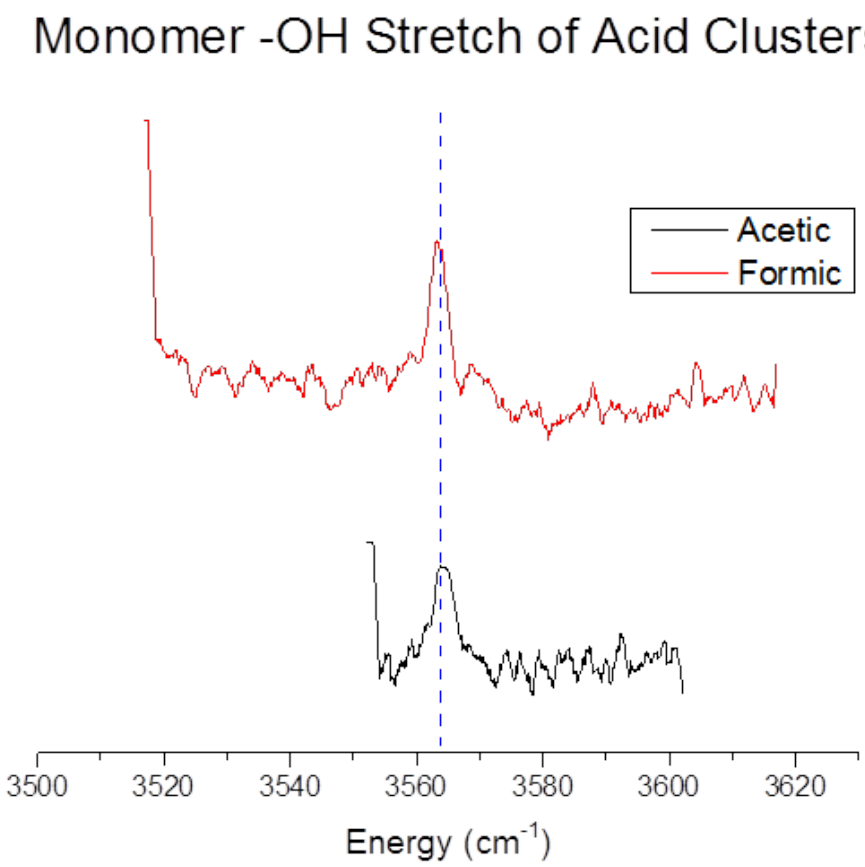

Figure 15: 4-AE -OH stretches of the formic and acetic acid clusters. Note the position and width of the peaks.

The propionic acid cluster did not exhibit any IR depletion from the 4⁻AE ⁻OH stretch in the tested range. The propionic acid did not have an IR depletion peak near or at 3,563.5 cm^{-1} as would be expected if the propionic cluster had the ring conformation. The gauche conformation predicts a 4⁻AE –OH stretch of 3524 cm^{-1} which was also not seen in the experimental data for the propionic acid. Attempts were made to obtain an IR signal for the propionic acid clusters over a range of 3502 cm^{-1} and 3622 cm^{-1}. The majority of the minimum energy structures from the calculations suggest that the –OH stretch for the 4⁻AE hydroxyl group in the cluster would appear in this range for the propionic acid cluster. All of the calculated structures predict a similar intensity for the 4⁻AE –OH stretch for the propionic and other acids. The observed 4⁻AE –OH stretch of the formic and acetic acid clusters

suggests that the intensity of the stretch and the experimental set-up were not the reason that repeated attempts in the range of 3,502 cm^{-1} and 3,622 cm^{-1} failed to find a peak for the propionic acid cluster. The minimum energy structure with the propionic acid over the ring, which could only be found using the MP2 and M06-2X methods, is the only structure which predicts a very different shift of the 4–AE -OH stretch which could explain the absence of the stretch in the tested range. Scaling factors for vibrational frequencies using MP2 and M06-2X methods with the 6-311++G(d,p) basis set were not found in the NIST database. The scaling factors for these methods using slightly different basis sets were recorded around 0.95.[24] The frequencies of the structure were also calculated using the B3LYP method for frequencies without the B3LYP geometry optimization. In all cases the 4–AE –OH stretch was predicted to be within 10 wavenumbers of the bluest –NH stretch of the molecule and is expected to be between 3,460 cm^{-1} and 3,500 cm^{-1}, which is outside of the tested experimental range. Continued experimentation of this range is necessary to further explore the possible structure of the propionic acid cluster. Currently, no information in the IR range is available to explain the structure of the propionic acid cluster.

The observed acid –OH stretch of the formic acid cluster supports the identification of the cluster as the ring conformation. The acid –OH stretch in the formic acid cluster is at 3,042 cm^{-1} which is much closer to the estimated 3,105 cm^{-1} of the ring structure than the estimated 3,172 cm^{-1} for the gauche structure. The IR depletion spectrum of the acid –OH stretch is shown in Figure **16**. The acid –OH

stretches were predicted to be considerably stronger than the 4-AE –OH stretches. The greatest percentage depletion of the signal was approximately the same for both –OH stretches when the peak of the signal was considered. The acid –OH stretch had a significantly wider peak and such a greater total depletion. The laser power in the dye region for the acid –OH stretch was much weaker also contributing to the signal strength of the acid –OH stretch. The dye laser was generating about half as much power which meant the generated IR was also decreased by about half. These experimental conditions made it difficult to observe the acid –OH stretch. The formic acid peak was reproducible.

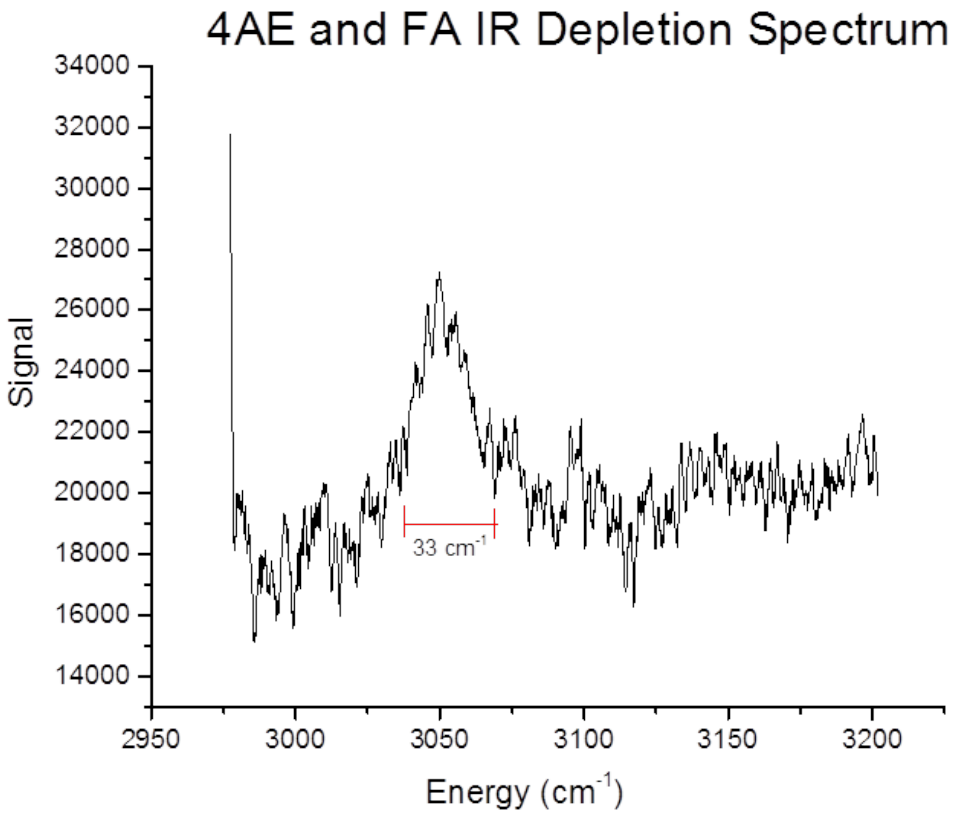

Figure 16: The formic acid cluster IR depletion scan of the acid –OH stretch. The peak is much broader and red shifted than the IR depletion peak of the 4-AE –OH stretch. The acid –OH bond is much weaker because the hydrogen is the acidic hydrogen of formic acid and it is heavily involved in the hydrogen bonding interaction of the cluster.

The acetic acid cluster also had a signal in the acid stretch range. Unlike the formic acid, the acetic acid IR depletion signal was not a single peak in the acid –OH stretch range. A three peak pattern was repeatedly seen for the acetic acid cluster. The IR depletion spectrum in Figure **17** is a sum of scans from the same day which shows the observed pattern. Summing the scans in the same conditions helps to increase the signal to noise of the spectrum. The depletion for even the largest of the peaks was modest, only about 35%, but was clearly a depletion and reproducible. The low amounts of IR power are part of the reason that the depletion level was low. The three peaks observed are likely a result of mixing of other vibrations with the acid –OH stretch. The shifted ⁻OH stretch frequency begins to overlap with the expected ⁻CH bands. The ⁻CH stretches typically have significantly smaller absorption cross sections but can borrow intensity from the ⁻OH stretch when they mix. This mixing tends to lower the overall strength of each individual band in this group leading to low amounts of total depletion. The acid –OH stretch was predicted to be very similar for the gauche and the ring conformation, only 17 cm^{-1} apart. This is not a large enough difference to provide any structure identification information based solely off the acid –OH stretch. The ring structure predicted the acid –OH stretch to be at 3,162 cm^{-1}. This is close to the range where the three depletion peaks are observed for the acetic acid –OH peak. The formic acid –OH stretch was predicted to be in a very similar place to the acetic acid –OH stretch in the gauche conformation but in the ring conformation the formic acid was expected farther to the red. This is seen

experimentally which supports the identification of both clusters as the ring conformation.

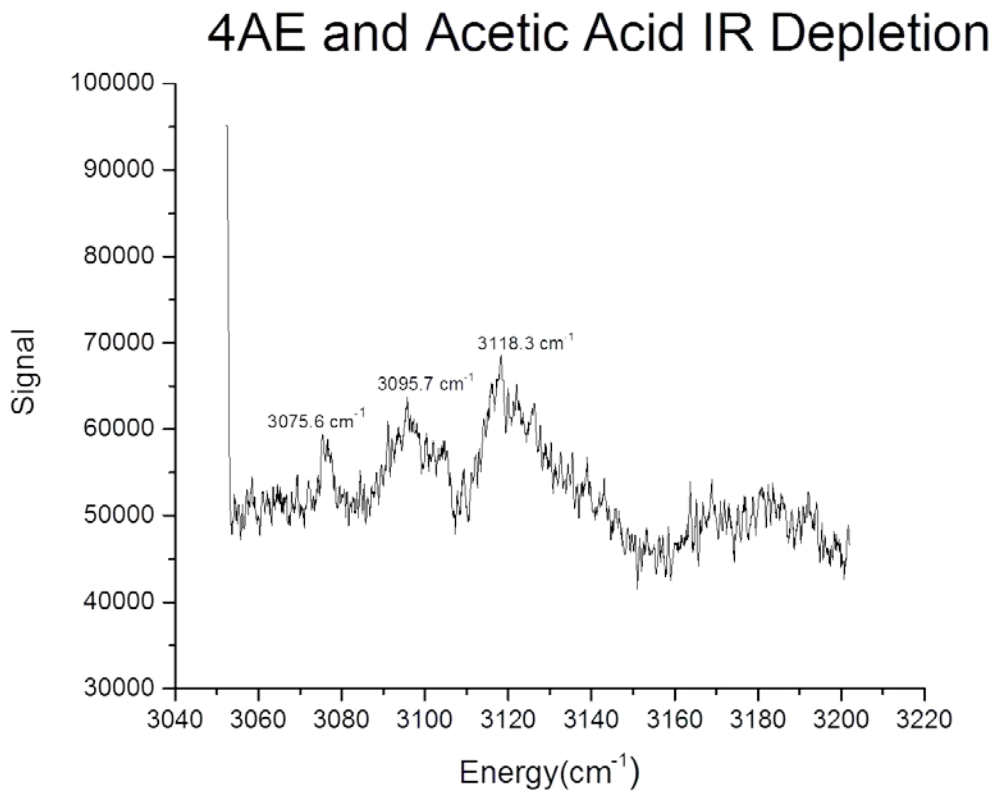

Figure 17: The acetic acid IR depletion spectrum for the acid –OH stretch. Unlike the other –OH stretches a single peak was not observed. Some weak signal was recorded for the range and it is likely a result of the acid –OH stretch. Combination bands with other nearby vibrations could explain the weak signal with multiple peaks. The three peak structure and relative position of the peaks was reproducible. The above figure is a sum of three scans all taken on the same day under identical conditions.

The propionic acid did not have an observable acid –OH stretch. This stretch was briefly searched for but the difficulty of measuring the acid –OH stretch did not allow a depletion signal to be observed. The measurement of the acid –OH peak relied on optimization of the IR depletion using the 4⁻AE –OH stretch for the other clusters. The lack of a 4⁻AE –OH peak for propionic acid made this optimization impossible and is likely the reason that an acid peak was not observed.

Conclusion:

A combination of experimental and computational techniques was used to determine the structure of the 4-AE monomer and some of its acid clusters. The use of calculations complimented the experimental data well and allowed conclusions to be drawn from the data. The 4-AE monomer was very clearly experimentally observed in two conformations. The dominant conformation is the gauche conformation while the secondary conformation was believed to be the anti conformation. To definitively identify the secondary conformation as anti the 4-AE –OH stretch needs to be measured. Interpretation of the cluster was not as straightforward and for the propionic acid the structure of the cluster was not determined. The experimental data for the formic acid cluster all pointed to the ring structure of the cluster which was also the favored conformation by the calculations. The acetic acid clusters could also be assigned using the experimental data. The 4-AE –OH stretch was the main clue in determining the structure of the acetic acid cluster using the predicted vibrational frequencies from calculations. The acetic acid 4-AE -OH stretch was in the same position as the formic acid -OH stretch. The calculations had predicted that the position of the 4-AE -OH stretch would only be in the same position for the acid clusters if they were all in the ring structure which, along with the positive identification of the formic acid cluster as the ring conformation, allowed the acetic acid cluster to be assigned as the ring structure. The propionic acid cluster REMPI spectrum has a red shift unlike the other acid clusters and no IR signal was able to be measured. There is a possibility the 4-AE –OH stretch is to the red of the

measured range. The differences in experimental behavior of the propionic and the other acids suggest that a different structure is present. Another attempt to measure the IR data for the –OH stretches of the propionic acid clusters is needed before any conclusions can be drawn about the propionic cluster. Further IR data can be gathered on the anti monomer conformation to undoubtedly identify this secondary monomer conformation as the anti conformation. Additional IR studies should be done in order to better understand the binding structure and strength of the clusters and 4⁻AE monomer. This data would allow the 4⁻AE to be compared to the 9HFCA more concretely and would complete the picture of the chromophore base.

References:

1. Smalley, R. E.; Wharton, L.; Levy, D. H., Molecular Optical Spectroscopy with Supersonic Beams and Jets. *Accounts of Chemical Research* **1977,** *10* (4), 139-145.
2. Johnston, M. V., Supersonic jet expansions in analytical spectroscopy. *Trends in Analytical Chemistry* **1984,** *3*.
3. Gu, Q., Unpublished work. **2015**.
4. J. C. Dean, N. L. B., J. R. Hopkins, J. G. Redwine, P. V. Ramachandran, S. A. mcLuckey, and T. S. Zwier, UV Photofragmentation and IR Spectroscopy of Cold, G⁻Type β⁻O⁻4 and β−β Dilignol−Alkali Metal Complexes: Structure and Linkage-Dependent Photofragmentation. *J. Phys. Chem. A* **2015,** *119*.
5. P. S. Walsh, E. G. B., J. R. Gord, and T. S. Zwier, Binding water to a PEG-linked flexible bichromophore: IR spectra of diphenoxxyethane-(H2O)n clusters, n = 2,4. *J. Phys. Chem.* **2015,** *142*.
6. J. C. Dean, R. K., P. S. Walsh, F. Allais, and T. S. Zwier, Plant Sunscreens in the UV-B: Ultraviolet Spectroscopy of Jet-Cooled

Sinapoyl Malate, Sinapic Acid, and Sinapate Ester Derivatives. *J. A. Chem.* **2014,** *136*.
7. N. L. Burke, J. G. R., J. C. Dean, S. A. McLuckey, and T. S. Zwier, UV and IR spectroscopy of cold protonated leucine encephalin. *International Journal of Mass Spectrometry* **2015,** *378*.
8. M. Mons, I. D., F. Piuzzi, B. Tardivel, and M. Elhanine, Tautomerism of the DNA Base Guanine and Its Methylated Derivatives as Studied by

Gas-Phase Infrared and Ultraviolet Spectroscopy. *J. Phys. Chem. A* **2002,** *106*.
9. Rizzo, T. R.; Park, Y. D.; Peteanu, L.; Levy, D. H., Electronic-Spectrum of the Amino-Acid Tryptophan Cooled in a Supersonic Molecular-Beam. *Journal of Chemical Physics* **1985,** *83* (9), 4819-4820.
10. Park, Y. D.; Rizzo, T. R.; Peteanu, L. A.; Levy, D. H., Electronic Spectroscopy of Tryptophan Analogs in Supersonic Jets - 3-Indole Acetic-Acid, 3-Indole Propionic-Acid, Tryptamine, and N-Acetyl Tryptophan Ethyl-Ester. *Journal of Chemical Physics* **1986,** *84* (12), 6539-6549.
11. Basu, S.; Knee, J. L., Vibrational dynamics of 9-fluorenemethanol using infrared-ultraviolet double-resonance spectroscopy. *Journal of Chemical Physics* **2004,** *120* (12), 5631-5641.
12. Gu, Q. L.; Knee, J. L., Binding energies and dissociation pathways in the aniline-Ar(2) cation complex. *Journal of Chemical Physics* **2008,** *128* (6).
13. Knee, Q. G. a. J. L., Communication: Spectroscopic measurement of the binding energy of a carboxylic acid-water dimer. *J. Chem. Phys.* **2012,** *136*.
14. Gu, Q. L.; Trindle, C. O.; Knee, J. L., Electronic and Cationic Spectroscopy of 9-Hydroxy-9-fluorene Carboxylic Acid. *Journal of Physical Chemistry A* **2014,** *118* (27), 4982-4987.

15. Wiley, W. C.; Mclaren, I. H., Time-of-Flight Mass Spectrometer with Improved Resolution. *Review of Scientific Instruments* **1955,** *26* (12), 1150-1157.
16. T. Wang, C. C., H. Hung, G. Kuo, and C. Han, Design parameters of dualstage ion reflectrons. *Review of Scientific Instruments* **1994,** *65*.
17. Frisch, J. B. F. a. A., *Exploring Chemistry with Electronic Structure Methods*. 2nd ed.; Gaussian Inc.: 1996; p 301.
18. Becke, A. D., Density-functional thermochemistry. III. The role of exact exchange. *J. Phys. Chem.* **1993,** *98*.
19. C. Lee, W. Y., and R. G. Parr, Development of the Colle-Salvetti correlation-energy formula into a function of the electron density. *Physical Review B* **1988,** *37*.
20. Truhlar, Y. Z. a. D. G., The M06 suite of density functionals for main group thermochemistry,

thermochemical kinetics, noncovalent interactions, excited states,

and transition elements: two new functionals and systematic testing

of four M06-class functionals and 12 other functionals. *Theor. Chem. Account* **2008,** *120*.
21. Simon, D. A. M. J. D., *Physical Chemistry: A Molecular Approach*. University Science Books: 1997.
22. Frisch, M. J. T., G. W.; Schlegel, H. B.; Scuseria, G. E.; Robb, M. A.; Cheeseman, J. R.; Scalmani, G.; Barone, V.; Mennucci, B.; Petersson, G. A.; Nakatsuji, H.; Caricato, M.; Li, X.; Hratchian, H. P.; Izmaylov, A. F.; Bloino, J.; Zheng, G.; Sonnenberg, J. L.; Hada, M.; Ehara, M.; Toyota, K.; Fukuda, R.; Hasegawa, J.; Ishida, M.; Nakajima, T.; Honda, Y.; Kitao, O.; Nakai, H.; Vreven, T.; Montgomery, Jr., J. A.; Peralta, J. E.; Ogliaro, F.; Bearpark, M.; Heyd, J. J.; Brothers, E.; Kudin, K. N.; Staroverov, V. N.; Kobayashi, R.; Normand, J.; Raghavachari, K.; Rendell, A.; Burant, J. C.; Iyengar, S. S.; Tomasi, J.; Cossi, M.; Rega, N.; Millam, N. J.; Klene, M.; Knox, J. E.; Cross, J. B.; Bakken, V.; Adamo, C.; Jaramillo, J.; Gomperts, R.; Stratmann, R. E.; Yazyev, O.; Austin, A. J.; Cammi, R.; Pomelli, C.; Ochterski, J. W.; Martin, R. L.; Morokuma, K.; Zakrzewski, V. G.; Voth, G. A.; Salvador, P.; Dannenberg, J. J.; Dapprich, S.; Daniels, A. D.; Farkas, Ö.; Foresman, J. B.; Ortiz, J. V.; Cioslowski, J.; Fox, D. J., Gaussian 09, Revision A.1. 2009.
23. Xu, Z.; Smith, J. M.; Knee, J. L., High-Resolution Threshold Photoelectron-Spectroscopy of Aniline and Aniline Vanderwaals Complexes. *Journal of Chemical Physics* **1992,** *97* (5), 2843-2860.
24. NIST Precomputer Vibrational Scaling Factors. http://cccbdb.nist.gov/vibscalejust.asp.